Authors' copy: A. Trkov, R. Capote et al, *Nuclear Data Sheets* **112** (2011) 3098-3119

# Covariances of evaluated nuclear cross-section data for $^{232}$Th, $^{180,182,183,184,186}$W and $^{55}$Mn

A. Trkov,[1] R. Capote,[2] E.Sh. Soukhovitskii,[3] L.C. Leal,[4] M. Sin,[5] I. Kodeli,[1] and D.W. Muir[6]

[1] *Jožef Stefan Institute, Jamova 39, 1000 Ljubljana, Slovenia*
[2] *NAPC–Nuclear Data Section, International Atomic Energy Agency, P.O. Box 100, A–1400 Vienna, Austria**
[3] *Joint Institute for Power and Nuclear Research – Sosny, BY-220109 Minsk, Belarus*
[4] *Oak Ridge National Laboratory, P.O. Box 2008, Oak Ridge, TN 37831-6171, USA*
[5] *Nuclear Physics Department, Bucharest University, 077125 Bucharest-Magurele, Romania*
[6] *Special Term Appointee Argonne National Laboratory, 9229 Rosewater Lane, Jacksonville, FL 32256, USA*

(Received 15 July 2011)

The EMPIRE code system is a versatile package for nuclear model calculations that is often used for nuclear data evaluation. Its capabilities include random sampling of model parameters, which can be utilised to generate a full covariance matrix of all scattering cross sections, including cross-reaction correlations. The EMPIRE system was used to prepare the prior covariance matrices of reaction cross sections of $^{232}$Th, $^{180,182,183,184,186}$W and $^{55}$Mn nuclei for incident neutron energies up to 60 MeV. The obtained modelling prior was fed to the GANDR system, which is a package for a global assessment of nuclear data, based on the Generalised Least-Squares method. By introducing experimental data from the EXFOR database into GANDR, the constrained covariance matrices and cross-section adjustment functions were obtained. Applying the correction functions on the cross sections and formatting the covariance matrices, the final evaluations in ENDF-6 format including covariances were derived. In the resonance energy range, separate analyses were performed to determine the resonance parameters with their respective covariances. The data files thus obtained were then subjected to detailed testing and validation. Described evaluations with covariances of $^{232}$Th, $^{180,182,183,184,186}$W and $^{55}$Mn nuclei are included into the ENDF/B-VII.1 library release.

**Contents**



## I. INTRODUCTION

In the early days of nuclear technology the designers were relying on experimental mockups to test new concepts and optimize the geometry and material composition. With increasing costs of running versatile experimental facilities, together with stricter licensing requirements and increased computational power of modern computers, much of the role of the experiments has been taken over by computational models. Even the best and most accurate models can only be as good as the input data, so there is an increasing demand from nuclear research, industry, safety and regulatory bodies for best estimate predictions of system performance in terms of the design and operational parameters of nuclear re-

*Electronic address: r.capotenoy@iaea.org;roberto.capote@yahoo.com

actors, which are to be provided with their confidence bounds. Uncertainties propagated from evaluated microscopic neutron cross-section data are an important component needed to estimate the accuracy of predictions of such integral quantities. The concern about data uncertainties is also related to the need to ensure that nuclear power will continue to be safe, reliable and economically competitive with other alternative energy options. Modern nuclear reactor code systems are now able to accommodate nuclear data uncertainties (e.g. the TSUNAMI module of the SCALE system [1] or the SUSD3D code [2], interfaced to several commonly used deterministic transport codes) thereby providing further stimulus for their production. Along with the growing demand for evaluated nuclear data that include uncertainties and correlations, considerable progress was made in evaluation methodologies. Several subgroups of the NEA Working Party for Evaluation Co-operation (WPEC) have been working on the subject and technical reports have been published recently [3–6].

Addressing the above-mentioned data needs the Nuclear Data Section of the International Atomic Energy Agency (IAEA) actively supported several activities to develop consistent methodologies for evaluating cross-section data including covariances. There is no uniquely correct way of doing this, but the resulting methodology discussed in the present contribution is based on a hybrid approach [4, 7]: modelling uncertainties are incorporated into the model prior, which is calculated stochastically within the EMPIRE code system [8]. Experimental data are incorporated into the evaluation by the Generalized Least-Squares (GLSQ) method as implemented within the GANDR system [9]. The hybrid evaluation method that combines properly-weighted experimental and model covariance matrices was the basic tool in the evaluations of the nuclear reaction data of $^{232}$Th, W-isotopes and $^{55}$Mn that includes full covariance information as will be shown below. The choice of the nuclides was driven by specific needs and outstanding deficiencies in the existing data as discussed in several IAEA projects. More detailed information for each studied case will be given in the sections that follow.

### A. Overview of the evaluations

The EMPIRE system [8] is quite flexible in the ways that prior covariance information can be generated. The approach adopted by an informal international consortium under the umbrella of the IAEA is described herein. The first material to be evaluated by this methodology was $^{232}$Th within the scope of the IAEA Co-ordinated Research Project (CRP) on "Evaluated nuclear data for Th-U fuel cycle" [10]. The evaluation included valuable contributions from different members of the CRP and was truly an international effort. The key point was the inclusion of integral benchmarks into the evaluation loop. In this way the sensitivities to various model parameters could be assessed early in the evaluation stage. Fine tuning of the input model parameters using integral data (within parameters' uncertainties estimated by expert judgement) was in some cases possible, where differential measurements were insufficient to determine the cross sections more precisely. It should be noted that parameters' variations based on integral data were introduced manually and no integral data were considered in the least-squares fit by GANDR. Within the same IAEA CRP, evaluated data files for $^{231,233}$Pa were also produced, albeit with less rigour because of a poorer experimental database available for these two isotopes. All three evaluations were adopted for the ENDF/B-VII.0 library [11]. Since then, minor changes to the cross sections of $^{232}$Th were made due to a slight refinement of the assigned correlations to the experimental data. $^{231,233}$Pa covariance evaluations were removed during the review process of the ENDF/B-VII.1 beta evaluations as they were considered of lower quality due to the scarcity of available experimental data, and they are not important for current applications.

Subsequently, the evaluations for the five naturally-occuring isotopes of tungsten were started. The evaluation for $^{180}$W was the first of its kind. Preliminary results were published at the ND2007 conference in Nice [12], and the files performed quite well on the FNG-W benchmark from the SINBAD compilation [13]. Extending the suite of benchmarks to the critical assemblies from the ICSBEP compilation [14] revealed that the benchmarks are sensitive to capture in the 100 keV range, similarly to the FNG-W benchmark, but with opposite indication: the ICSBEP criticality benchmarks over-predicted the reactivity and required an increase in capture while the FNG-W underpredicted the activation of gold foils in a tungsten block and required a decrease in capture. The evaluation procedure was therefore an iterative process of fine-tuning the capture and other cross sections in different energy regions to retain good performance for the FNG-W benchmark, and at the same time improve the performance in the ICSBEP benchmarks. The results of this iterative process were presented at Port Jefferson in 2008 [15]. Since then, only minor changes to the evaluated nuclear data files were made. For example, an error was removed in the assigned gamma-width of the $^{184}$W resonance at 1132 eV, which was discovered through benchmarking, and a few small changes were made to the covariance data for consistency with integral observables.

Very recently the evaluation of the reaction cross-section data of $^{55}$Mn was performed using the same methodology. Detailed results are presented in the sections that follow.

## II. COVARIANCE EVALUATION METHODOLOGY

### A. Resonance region

The EMPIRE system has an in-built capability to produce resolved resonance files with covariances from the information available in the Atlas of Neutron Resonances by Mughabghab [16]. This option is commonly applied in the evaluations produced at the National Nuclear Data Center at the Brookhaven National Laboratory. In our case we preferred to use the resonance data with covariance information obtained directly from the analysis of the transmission and capture measurements, when possible. In all discussed cases the resonance evaluations from the Oak Ridge National Laboratory (ORNL) were adopted. The $^{232}$Th resonance data represent a new evaluation that includes the covariance information [17]. Resonance parameters of the tungsten isotopes were taken from existing evaluations with minor adjustments and the covariance information was generated by the retroactive method [18] because insufficient new measurements were available to justify a re-evaluation. Since then, new measurements have been completed at the IRMM laboratory in Geel [19] and analysis is in progress at ORNL, but is not expected to be finalised in a short time and is not included in the present work. The $^{55}$Mn resonance data including uncertainties are the result of a new evaluation performed at ORNL [20], including the covariance information.

### B. Fast neutron region: Uncertainty of the reaction models and model-parameter uncertainties

In the fast energy region (i.e. above the resonance region) the covariance information is prepared in two steps. In the first step the covariance prior is generated by a Monte Carlo technique based on a random sampling of model parameters and subsequent nuclear model calculations using the EMPIRE code [8]. In the second step the calculated cross sections and the corresponding covariance matrix generated from parameters' sampling in model calculations are fed as a prior information to the GANDR system that combines it with selected experimental data as described in the next Section.

A brief description of the reaction modelling relevant for covariance calculations is given next. Readers interested in a detailed description of theoretical modelling are referred to a companion paper by Chadwick *et al.* [21]. It is well established that a set of optical model potential (OMP) parameters that can reproduce the nucleon scattering data over a wide energy range is essential for reliable nuclear data predictions. All IAEA evaluations in the fast neutron range described in this contribution have been based on newly derived coupled-channel optical model potentials using dispersion relations (see Refs.[22, 23] and references therein). Starting values for nuclear model parameters and their uncertainties were taken from the RIPL recommendations [23, 24]. Pre-equilibrium emission was considered using a one-component exciton model (PCROSS), which includes nucleon, gamma and cluster emission. Hauser-Feshbach [25] and Hofmann-Richert-Tepel-Weidenmüller [26] versions of the statistical model were used for the compound nucleus cross-section calculations. Both approaches account for the multiple-particle emission and the full gamma-cascade. Level densities were described by the "EMPIRE specific" formalism, which uses the superfluid model below the critical excitation energy and the Fermi gas model above [8, 23]. A modified Lorenzian (MLO) radiative-strength function was taken as recommended by Plujko [23].

The use of model calculations to the determination of covariances for the nuclear reaction observables is very transparent [27]. First, physical model parameters that play a significant role in defining reaction observables of interest are identified. A typical list of model parameters with assigned uncertainties used to calculate the model prior uncertainties for the $^{232}$Th evaluation is given in Table I of Section III.A. The number of sampled parameters is case-dependent. Usually we include level density parameters for the target and compound nuclei as well as for selected residual nuclei of major competing channels. Other parameters of the reaction model such as the exciton model mean-free path (pre-equilibrium parameter with assumed relative uncertainty of 30%) and optical model parameters (e.g. potential depth, geometric parameters, static and dynamic deformation) are also considered. Adopted model parameter uncertainties are usually those recommended in the RIPL database [23]. Additionally, scaling (or normalisation) parameters (e.g. of the total and the reaction cross sections) with empirically estimated uncertainties take into account systematic deficiencies of nuclear-reaction models. Scaling (non-physical) parameters may be energy dependent, in which case they are assumed to be fully correlated between different energies. The assumption of fully-correlated scaling parameters is required to avoid fluctuations of calculated cross sections at different energies, i.e. the relevant cross section is scaled but the model shape is preserved. A typical uncertainty of scaling parameters is small: 3%. Once all random variables (parameters) and their corresponding uncertainties are defined, then the EMPIRE code is run for a number of times. Previously selected input parameters are being sampled randomly within the assumed uncertainty around the central (nominal) values of the parameters [28]. A normal distribution of the parameters is assumed; the uncertainty of the parameters is limited to 33 % (if needed) to reduce the number of sampled negative values, which are often unphysical and are discarded. Physical model parameters are assumed to be independent as parameters' correlation does not have a significant impact on already very strong correlation arising from the nuclear reaction model. Sampling of correlated physical parameters is avoided (either the

potential depth or the potential radius is sampled, never both of them).

Each EMPIRE calculation with a different set of sampled random parameters covers the full incident energy range and produces a full set of cross sections, spectra, angular distributions and other observables. EMPIRE also produces a full ENDF-6 formatted file for each of the sampled sets. Variances and covariances of any cross section $x$ (including the double differential ones) or other parameters can be obtained from the randomly sampled values $x_k$ of the cross section $x$ by

$$\mathrm{Cov}(x_i, x_j) = \frac{1}{N} \sum_{i,j=1,N} (x_i - \overline{x})(x_j - \overline{x}) \qquad (1)$$

where $N$ is the number of samples and $\overline{x}$ is the average over $N$ sampled values of $x_k$. The amount of information that needs to be stored should remain reasonable and there are some restrictions in the ENDF-6 format itself, so we choose the energy grid points at which the cross sections are sampled and reaction definitions as commonly used in the GANDR system [9]. This implies that all reactions are given on the same energy grid and that some reactions are lumped together to reduce the size of storage of information. Cross correlations between different reactions are automatically taken into account. The GANDR system works in the cross-section space and does not keep track of the input model parameters.

Energy-range correlations of the model covariance for each reaction are typically very strong and generally positive (at least on the short range), reflecting the stiffness of nuclear reaction models. Such property of the modelling covariance matrix is very general, and is related to the small number of model parameters used to describe a very big number of experimental data points. A typical model correlation matrix for the $^{186}W$(n,$\gamma$) produced by random sampling is shown in Figure 1. Strong positive correlations are observed even between distant energy points. Correlations are weakened when experimental data are considered by GANDR as seen in Figure 2 (see the next section for further discussion of the GANDR fit).

The Monte Carlo calculated uncertainty as a function of energy for the $^{186}W$(n,$\gamma$) reaction is shown as a dashed line in Figure 3. The prior uncertainty goes from 20%–30% below 1 MeV up to 60% in the energy region of 2–10 MeV. Higher uncertainty above 3-4 MeV results from more competing channels open, with the capture contribution becoming negligible compared to competing channels at higher energies. Uncertainty of 20%–30% below 1 MeV is mainly related to the assumed uncertainty of the level density parameter of the compound nucleus, determining the normalization of the capture cross section at low energies.

The Monte Carlo (MC) calculations defining the prior covariance matrix are conceptually straightforward and free of many simplifying assumptions used in deterministic methods, in particular of the assumption of a linear response of the observables to the variation of model pa-

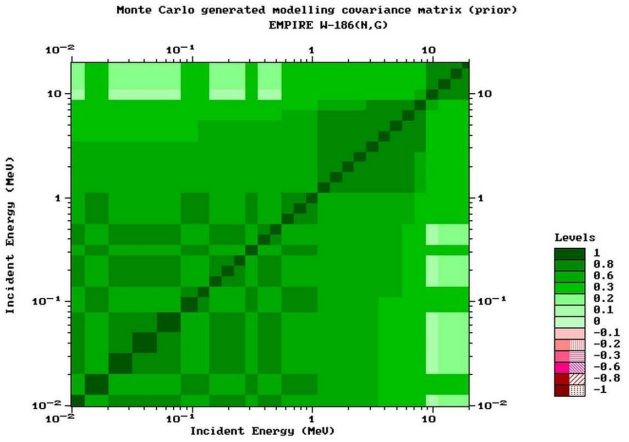


FIG. 1: Correlation matrix of the $^{186}$W(n,$\gamma$) Monte Carlo prior.

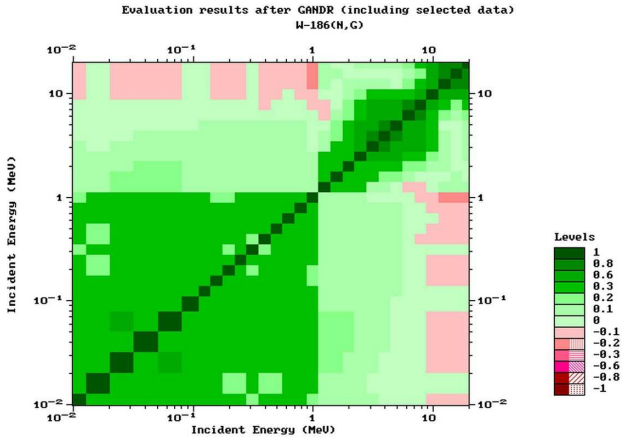


FIG. 2: Correlation matrix of the $^{186}$W(n,$\gamma$) after the GANDR fit.

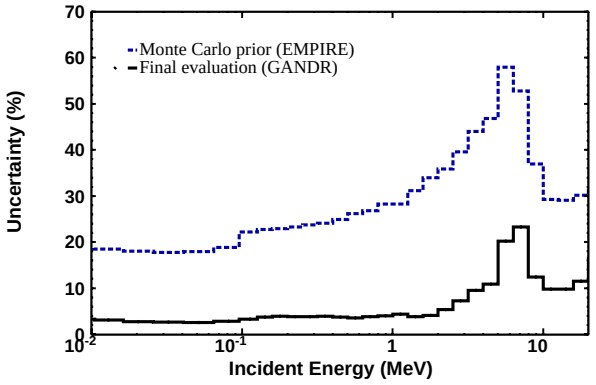


FIG. 3: Uncertainty of the $^{186}$W(n,$\gamma$) reaction in the fast neutron region: Monte Carlo calculated prior with EMPIRE (dashed line) is compared with the evaluation derived by GANDR result (solid line).

rameters [4], which is inherent in the least-squares methods (e.g. KALMAN [29]). There is also no need in MC methods to calculate the sensitivity coefficients, and the computing time is independent of the employed number of model parameters. These advantages come at a price – the number of required MC calculations is in the range of hundreds and the convergence of the results has to be demonstrated.

MC and deterministic methods for generation of the prior information are independent and complementary: the model-based covariances generated by the MC method can be used as a reference benchmark case for validating the faster but linear-model calculations with least-squares codes such as KALMAN.

### C. Combining modelling uncertainty and experimental data: the GANDR system

In the second step the calculated cross sections and the corresponding covariance matrix generated from parameters' sampling in model calculations are fed as a prior information to the GANDR system. An alternative to the two-step approach with GANDR would be to use the Unified Monte Carlo method (UMC) [30] in which both the model parameters and the experimental data are sampled together. The UMC method was demonstrated to work efficiently [31, 32] and is free from the effects of nonlinearities, but it is computationally very intensive and needs some additional development for a broad scale application. It should be also remarked that the results of the UMC method converge to the results of the GLSQ method if no experimental ratio data are involved in the evaluation [31].

A careful selection of available experimental data is made (from EXFOR [33]); the experimental data are renormalised to the most recent standards (if needed) or corrected for known deficiencies. Great care is devoted to the assembly of the experimental database that is statistically consistent as least-squares methods have inherent problems in dealing with discrepant data. Unknown experimental uncertainty components are added using expert judgement, if applicable. An estimate of the systematic relative uncertainties is made, separately for the data points from the same measurement and for the data sets from different measurements of the same reaction. Cross correlations between different measurements for the same reaction channel are defined by grouping experiments according to the employed measurement technique (e.g. activation, time-of-flight, etc). Experimental cross correlations between measurements for different reaction channels are not considered, which is probably a reasonable assumption, since the measurement techniques are usually quite different (an exception may be those activation measurements of different reactions undertaken at the same experiment). The selected experimental data are fed into the GANDR system and the adjustment of the cross sections and the covariance matrix is made by the GLSQ method for each reaction in turn. This can be done without loss of generality since the cross-reaction correlations from model calculations are already included in the prior, and a subsequent addition of experimental data is allowed within the bayesian approach as long as added experimental data are uncorrelated.

The average (nominal) model parameters in the reference EMPIRE calculation are chosen such that they reproduce relatively well the bulk of the experimental data. Therefore, the correction factors for the cross sections after the GANDR least-squares adjustment are generally small (i.e. close to one). The adjustments factors and the covariance matrix are obtained from the GANDR output. Adjusted cross sections and the corresponding covariance matrix are written to the final ENDF-6 file.

Strong energy-range correlations of the prior (model) covariance are significantly softened when experimental data are considered in a Generalized Least-Squares fit by GANDR system. Some anticorrelation of fitted data at distant energies are usually observed as seen in Figure 2, showing the correlation matrix of the evaluation produced by GANDR for the $^{186}W$(n,$\gamma$) reaction. Experimental data considered in the fit are described in a relevant section below. A different behavior of the correlation pattern is observed below and above 1 MeV. Below 1 MeV long-range correlations are still quite strong as they were in the prior covariance (see Figure 2). Above 1 MeV correlations became short-range (in fact a quasi-diagonal matrix is obtained). Additionally, anticorrelations are observed between higher and lower energy regions.

The uncertainty of the evaluated data as a function of energy for the $^{186}W$(n,$\gamma$) reaction is shown as a solid line in Figure 3. It can be seen that evaluation uncertainties are reduced to 3-4% below 1 MeV from the 20%–30% given for the model prior. This is a direct result of including accurate experimental data in the GANDR fit for this energy region. Uncertainty of the capture cross section is also reduced from 60% (prior) to 20% (final evaluation) for the energy region from 5-10 MeV. There is practically no experimental data available in this energy region. However, strong long-range model correlations from the prior combined with accurate experimental data below 1 MeV lead to the observed uncertainty reduction. There is some additional experimental data around 14 MeV allowing for a further reduction of the capture uncertainty at those higher energies.

Summarizing, we can say that model correlations from the calculated prior define the approximate shape of the evaluated cross sections (including the case when no experimental data are available). On the other side, the existence of accurate and statistically consistent (non-discrepant) experimental data is necessary to obtain cross-section uncertainties of the final evaluation below 10%.

### D. Cross-reaction and cross-material covariances

Since all cross sections at the specified energy grid-points are packed into a single parameter array, the cross-reaction covariances are produced naturally by GANDR. The parameter array can also contain Legendre moments of the angle-differential scattering cross section, as well as particle emission spectra. The first angular moment of the elastic cross section and the first angular moment of the first discrete level inelastic cross section are taken into account, which can be stored in the ENDF-6 format as covariances of the first-order Legendre coefficient of the same reaction in the laboratory system, but without correlations with other reactions. Covariances of the emission spectra were not taken into account in the present work (even if they are present in the prior covariance). However, it should be noted that neutron emission spectra are naturally correlated to corresponding cross sections; a fact which may be important for criticality calculations. Further studies of these correlations in future evaluations are warranted.

The most recent version of GANDR can treat experimentally measured elemental cross sections in combination with isotopic cross sections. For tungsten isotopes there are measured total cross-section data available both for the natural element and major isotopes. The inclusion of measurements on natural element in the GLSQ fit leads to cross-material correlations between the evaluated cross sections for different isotopes. Preliminary calculations were made exploiting this option in the case of the tungsten isotopes, but the cross-material covariances were not included in the final evaluation. However, it should be noted that the availability of experiments for all major isotopes of multi-isotopic elements is quite unique; usually only the elemental data exist and derived correlation among different isotopes seem unavoidable in future evaluations of important multi-isotopic elements (e.g. zirconium, iron, lead).

### E. Covariance formats and data processing

In general, the ENDF-6 convention is that the total cross section is a redundant reaction. Some evaluators argue that this is the best-known experimental cross section and should be given explicitly, but this is not how the total cross section is usually used in the calculations. The GANDR convention is consistent with the ENDF-6 convention that the total cross section is redundant and that the uncertainty in the total cross section can be reconstructed from the partials. In this process it is critical to account properly for cross-reaction correlations, otherwise the uncertainty in the total cross section could be overestimated (obviously some of the contributing reactions are always anticorrelated). For the same reason it is also important that all reactions that constitute the total cross section are accounted for. To keep the covariance information within reasonable limits in size, reactions are often lumped together. A typical case is the lumping of a number of discrete level reactions. Another example are the two-neutron and three-neutron emission reactions, which are lumped conveniently for transport calculations. This structure could confuse some users, who would be seeking the uncertainty in the (n,2n) reaction, for example. Such a user should be aware that a distinction between the lumped reaction and the (n,2n) covariances occurs only above the threshold for the (n,2n+p) reaction, and similarly for the three-neutron emission case.

The covariances for all reactions in the fast energy range are stored as the upper-triangular relative covariance matrix (Option LB=5 of File 33 in ENDF terminology). In the resonance range the resonance parameter covariances are stored in ENDF-6 File 32. A background uncertainty in the resonance range is also given in some cases. This option is used to account for sources of uncertainty not included in the resonance parameters' part. Most commonly this includes the scattering radius uncertainty (which could not be accomodated into the resonance covariances because the relevant ENDF-6 format extensions were introduced recently), but also some other systematic uncertainties. It should be noted that the use of File 32 allows for the storage of the full correlation information, and facilitates an accurate calculation of the uncertainty of the integral quantities (e.g. the resonance integral with a high level of self-shielding) as demonstrated in a recent paper by some of the authors [34].

## III. EVALUATION OF THORIUM

### A. EMPIRE model calculations

The details of the selection of optical model and other parameters for calculating the cross sections in the fast energy range are described in a separate paper [21]. The choice of model parameters may include tuning (scaling) factors, which are used to compensate for the deficiencies of the models to represent the cross sections. The list of model parameters and their uncertainties are listed in Table I; OMP means optical model potential. It is worth to remark that OMP depths are sampled, but not the OMP radii to avoid a well known model correlation. The average value of the parameters is chosen empirically following RIPL guidelines [23].

The full covariance matrix corresponds to a vector of parameters, which consists of cross sections, packed into the vector one after the other. Some of the cross sections in the vector represent lumped reactions. The definitions of each cross-section set in the vector is given in Table II. Note that the energy grid is fixed and is the same for all reactions, but some reactions require fewer points due to their respective thresholds.

To generate the covariance matrix prior, all model parameters in Table I were sampled randomly (and independently) using a normal distribution. From each set of

TABLE I: Model parameters with assigned uncertainties for $^{232}$Th evaluation. Target: $^{232}$Th; compound: $^{233}$Th; proton emission residual: $^{232}$Ac; alpha emission residual: $^{229}$Ra. Column "Symbol" designates the EMPIRE keyword for the respective parameter.

| EMPIRE input parameter | Symbol | Value | Unc. [%] | Nucleus |
|---|---|---|---|---|
| Preeq. mean-free path | PCROSS | 1.6 | 12 | |
| Level density normalization | ATILNO | 0.872 | 15 | $^{233}$Th |
| Level density normalization | ATILNO | 1.091 | 10 | $^{232}$Th |
| Level density normalization | ATILNO | 0.982 | 5 | $^{231}$Th |
| Level density normalization | ATILNO | 1.042 | 5 | $^{230}$Th |
| Level density normalization | ATILNO | 0.962 | 5 | $^{229}$Th |
| Level density normalization | ATILNO | 1.091 | 10 | $^{227}$Th |
| Level density normalization | ATILNO | 1.022 | 10 | $^{226}$Th |
| Level density normalization | ATILNO | 1.061 | 10 | $^{225}$Th |
| Level density normalization | ATILNO | 1.041 | 10 | $^{232}$Ac |
| Level density normalization | ATILNO | 1.041 | 10 | $^{231}$Ac |
| Level density normalization | ATILNO | 1.041 | 10 | $^{230}$Ac |
| Preeq. level density normal. | GTILNO | 1.05 | 10 | $^{232}$Ac |
| Preeq. level density normal. | GTILNO | 1.05 | 10 | $^{229}$Ra |
| Gamma-width normalization | TUNE | 3.3 | 5 | $^{233}$Th |
| Dynamic-deformation normal. | DEFDYN | 1.0 | 15 | $^{232}$Th |
| Fission barrier normalization | | 1.0 | 5 | all |
| Fission level density normal. | ATILFI | 1.0 | 5 | all |
| Real vol. OMP depth normal. | UOMPVV | 1.0 | 3 | $^{232}$Th |
| Imag.vol. OMP depth normal. | UOMPWV | 1.0 | 5 | $^{232}$Th |
| Imag.surf. OMP depth normal. | UOMPWS | 1.0 | 5 | $^{232}$Th |
| Vol. OMP diffuseness normal. | UOMPAV | 1.0 | 2 | $^{232}$Th |
| Surf. OMP diffuseness normal. | UOMPAS | 1.0 | 3 | $^{232}$Th |
| Real vol. OMP depth normal. | UOMPVV | 1.0 | 3 | $^{231}$Th |
| Imag.vol. OMP depth normal. | UOMPWV | 1.0 | 5 | $^{231}$Th |
| Imag.surf. OMP depth normal. | UOMPWS | 1.0 | 5 | $^{231}$Th |
| Vol. OMP diffuseness normal. | UOMPAV | 1.0 | 5 | $^{231}$Th |
| Surf. OMP diffuseness normal. | UOMPAS | 1.0 | 5 | $^{231}$Th |

sampled parameters a full ENDF-6 file was generated. In total 283 files were produced. Relevant cross sections were extracted from the files and lumped reaction cross sections were constructed. The cross sections were packed into the cross-section parameter vector. Using Equation (1) the elements of the covariance matrix were generated.

To account for additional unidentified uncertainties in the thorium evaluation, the variance of the prior was scaled by a factor of two. The scaling is arbitrary and may reduce excessively the correlations from the model parameters in some cases. This practice was changed in newer evaluations. However, the final variances are determined through the adjustment procedure by the method of generalised least squares, so the influence of this practice on the final results was considered less important.

### B. Selection of experimental data

Experimental data were retrieved from the EXFOR database [33] for the fission, (n,2n), radiative capture and total cross sections. Each data set was carefully reviewed. Whenever possible, measured cross sections were renormalised to the latest standards, or corrected otherwise, if justified. Measurements that were deemed unreliable were rejected.

Fission cross-section measurements included in the analysis are listed in Table III. Since practically all measurements were measured as ratios to a chosen standard, a 2 % fully correlated uncertainty was added to all measurements.

Measured (n,2n) and radiative capture cross sections included in the analysis are listed in Tables IV and V.

The adopted total cross-section measurements are listed in Table VI. Although the total cross section does not appear explicitly in the list of reactions, it is the sum of all the partial cross sections. The measurements act as a constraint on the sum. Although the measured uncertainties are quoted as total, a 1 % systematic uncertainty was acknowledged by Abfalterer *et al.* in recent publications [35, 36]. Similar analysis is missing in other experimental reports, therefore 1 % systematic uncertainty is adopted by analogy for all measurements, considering that all measurements were done using the time-of-flight method. In addition, a 0.2 % fully correlated uncertainty was assumed between all measurements.

The covariance matrix prior and the above-listed experimental data were entered into the GANDR system and GANDR was run to calculate the adjustment factors

TABLE II: Cross-section definition in the parameter covariance vector in terms of the ENDF-6 reaction designation MT numbers. The Npnt column designates the number of energy points.

| Npnt | Contributing MTs (description) |
|---|---|
| 74 | 2 (elastic) |
| 74 | $P_1$(2) (first moment of the elastic) |
| 74 | $P_2$(2) (second moment of the elastic) |
| 74 | $P_3$(2) (third moment of the elastic) |
| 13 | 5 |
| 16 | 16 24 41 (lumped) |
| 14 | 17 |
| 36 | 51 (first discrete inelastic) |
| 36 | $P_1$(51) (first moment of 51) |
| 32 | 52 53 54 55 56 57 58 59 60 |
| 25 | 61 62 63 64 65 66 67 68 69 |
| | 70 (lumped) |
| 28 | 22 28 71 72 73 74 75 76 77 |
| | 78 79 80 81 82 83 84 85 86 |
| | 87 88 89 91 (lumped) |
| 74 | 102 |
| 74 | 18 |
| 22 | 600 649 800 849 (lumped) |

TABLE III: Selection of $^{232}$Th(n,f) cross-section measurements from the EXFOR database.

| EXFOR No. | Author | Year | Comment |
|---|---|---|---|
| 41455006 | Shcherbakov *et al.* | (2001) | Ratio |
| | Eismont *et al.* | (1999) | Priv. comm. |
| 31424002 | Sastry *et al.* | (1992) | |
| 31459025 | Garlea *et al.* | (1992) | |
| 41111002 | Fursov *et al.* | (1991) | Ratio |
| 14176006 | Lisowski *et al.* | (1988) | |
| 40888002 | Goverdovskij *et al.* | (1986) | Ratio |
| 21963002 | Kanda *et al.* | (1985) | Ratio |
| 30813007 | Garlea *et al.* | (1984) | |
| 10658002 | Behrens *et al.* | (1982) | Ratio |
| 20796002 | Blons *et al.* | (1975) | |
| Systematic uncertainties: | | | |
| 2 % | common to all measurements | | |

TABLE IV: Selection of the $^{232}$Th(n,2n) reaction cross-section measurements from the EXFOR database.

| EXFOR No. | Author | Year | Comment |
|---|---|---|---|
| 22845002 | Karamanis *et al.* | (2003) | |
| 41240118 | Filatenkov *et al.* | (1999) | renormalized |
| 22235002 | Chatani *et al.* | (1993) | |
| 22637089 | Konno *et al.* | (1993) | |
| 22203002 | Chatani *et al.* | (1991) | |
| 30816002 | Raics *et al.* | (1985) | |
| 20499003 | Karius *et al.* | (1979) | |
| 12305002 | Cochran *et al.* | (1958) | |

for the cross sections by the GLSQ method. The covariance matrix of the adjustment factors is by definition the relative covariance matrix of the cross sections.

The adjustment factors were applied to the cross sections from the nominal EMPIRE calculation and the full covariance matrix was processed with a local code ENDCOV to create the final evaluated nuclear data file for $^{232}$Th.

In the resolved resonance range the resonance parameters were obtained from a sequential Bayes analysis [17, 37, 38] with the computer code SAMMY [39]. The experimental data base included Olsen [40] neutron transmission data (ORELA), Schillebeeckx [41] capture data (GELINA), and Gunsing [42] capture data (n_ToF) in the energy range 1 eV to 4 keV. In the thermal energy range the capture data of Chrien [43] and of Lundgren [44] were normalized to a value of 7.35 b recommended by Trkov [45] and fitted by SAMMY along with the total cross section of Olsen [40] in the energy range up to 1 eV. The covariances of the resonance parameters were obtained directly from the resonance analysis [17, 38]. They are stored in ENDF-6 File 32.

TABLE V: Selection of $^{232}$Th capture cross-section measurements from the EXFOR database.

| EXFOR entry | Author | Year | Comment |
|---|---|---|---|
| 22875002 | Schillebeeckx *et al.* | (2004) | |
| 22654003 | Wisshak *et al.* | (2001) | |
| 22663002 | Karamanis *et al.* | (2001) | |
| 41183003 | Davletshin *et al.* | (1993) | |
| 20871002 | Kobayashi *et al.* | (1979) | |
| 10735002 | Poenitz *et al.* | (1978) | |
| 10554003 | Macklin *et al.* | (1977) | |

TABLE VI: Selection of the $^{232}$Th total cross-section measurements from the EXFOR database.

| EXFOR No. | Author | Year | Comment |
|---|---|---|---|
| 13753029 | Abfalterer *et al.* | (2001) | |
| 12853052 | Poenitz *et al.* | (1983) | |
| 10935004 | Poenitz *et al.* | (1981) | |
| 21766002 | Iwasaki *et al.* | (1981) | |
| 10047094 | Foster Jr *et al.* | (1971) | |
| 21088003 | Uttley *et al.* | (1966) | |
| Systematic uncertainties: | | | |
| 1.0 % | for each EXFOR set | | |
| 0.2 % | correlation between all experiments | | |

The covariance matrix of the average resonance parameters in the unresolved resonance region (URR) was deduced from the covariance matrix of the experimental data and the sensitivity matrix or the partial derivatives with respect to the adjusted parameters [46]. The covariance matrix of the experimental data in the URR was constructed by assuming the following uncertainties:

Total cross section:
- correlated : 1.0 %
- uncorrelated : 0.5 %

Capture cross section
- correlated : 1.5 %
- uncorrelated : 1.5 %

The sensitivity matrix was deduced with the RECENT code of the PrePro series [47] around the final average resonance parameters. The covariance and sensivitivy matrix were constructed at the energy points of the tabulated cross-section data.

Since in the fitting procedure only the neutron strength functions $S_l$ for $l = 0, 1$ and 2 and the radiation widths $\Gamma_{g,l}$ for $l = 0, 1$ were adjusted, only the partial derivatives with respect to these parameters were considered. To construct the covariance matrix in File 32 a very small relative uncertainty on the level distance was introduced and it was assumed that the relative covariance elements for the reduced neutron widths can be approximated by the relative covariance elements of the neutron strength functions.

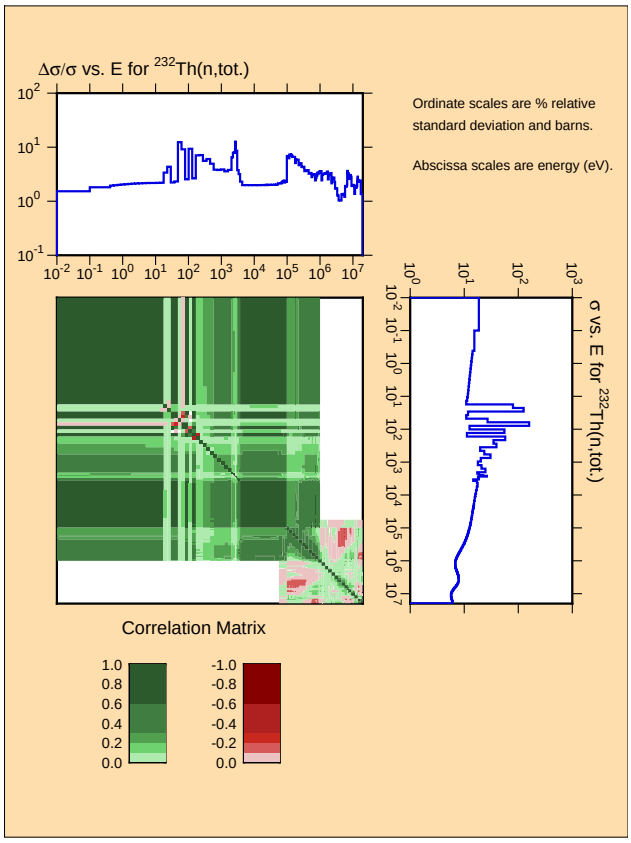


FIG. 4: Uncertainty and correlation matrix of the $^{232}$Th total cross section.

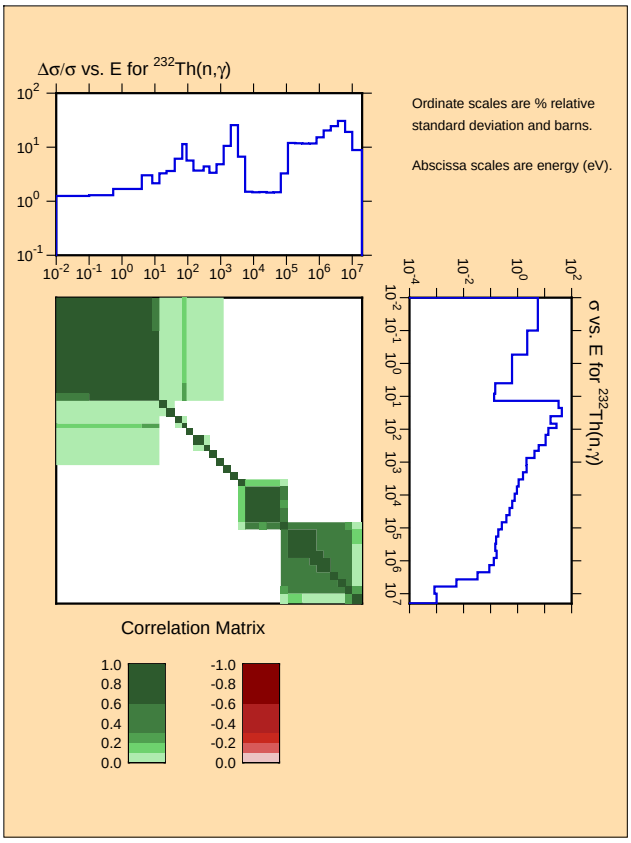


FIG. 5: Uncertainty and correlation matrix of the $^{232}$Th(n,$\gamma$) reaction.

A 2 % uncertainty was added from $10^{-5}$ eV to 897 keV to the elastic cross section in File 33 to account for the scattering radius uncertainty.

The data on the average number of neutrons per fission (including covariances) were adopted from the BROND-2 evaluation, which is based on a least-squares fit of selected experimental data sets.

### C. Analysis of obtained covariances

The full evaluated files with covariances were verified by the ENDF Utility Codes [48] to check for the formal correctness. In the next step the covariance plots were generated on a fine energy grid with the NJOY processing system [49] to check processability and the general features of the covariance matrices, including cross-reaction correlations. The covariance matrix of the total cross section is the sum of the covariance matrices of the partial reaction cross sections. The variance in the total cross section is smaller than the sum of the variances of the partials due to cross-reaction anti-correlations. The correlation matrix of the total cross section is shown in Figure 4 as an example of a derived result.

The next step in testing the covariance matrices was to generate with the NJOY code [49] the average capture cross sections in a thermal Maxwellian spectrum and the resonance integral in a pure $1/E$ spectrum from 0.55 eV to 2 MeV, including uncertainties, which can be compared to the values derived from the database of constants for neutron activation analysis recommended by the International Union of Pure and Applied Chemistry (IUPAC) [50]. The comparison is described in Table VII. The thermal capture cross-section uncertainty derived from the $k_0$ constants in the IUPAC database is lower because it does not include the systematic uncertainty in the gamma-emission probabilities. The resonance integral calculated from the evaluated cross sections is lower, but since the evaluation is based on two very recent data sets measured on GELINA at IRMM in Geel and on n_ToF at CERN in Geneva, which are in excellent agreement, we believe that the uncertainty estimate is reliable. Particularly, the accuracy quoted in Table VII is observed also in the unresolved resonance region. From Figure 5 it is evident that the uncertainties at the upper end of the resolved resonance range ( 10 eV to 4 keV) are mainly statistical (correlations are negligible) and contribute little to the total uncertainty of the resonance integral.

TABLE VII: Comparison of thermal capture cross section and resonance integral uncertainties of $^{232}$Th with values derived from constants for neutron activation analysis [50].

| | IUPAC/Nudat | | ENDF/B-VII.1 | | |
|---|---|---|---|---|---|
| | | Uncert. | | Uncert. | Difference |
| | [barns] | [%] | [barns] | [%] | [%] |
| $\sigma_0$ | 7.34 | 0.5 | 7.338 | 1.2 | 0.0 |
| RI | 84.64 | 3.6 | 84.23 | 1.9 | -0.5 |

## IV. EVALUATION OF TUNGSTEN ISOTOPES

### A. EMPIRE model calculations

As in the case of the $^{232}$Th nucleus, the details of the selection of optical model and other parameters are described in a separate paper [21]. The choice of model parameters includes tuning (scaling) factors to compensate for the deficiencies of the reaction models used to represent the cross sections. The absolute value of correction is always less than 5 %. These "non-physical" parameters could be energy dependent. It is important to realise that the values of tuning parameters at different energies are correlated. Full correlation was assumed when energy-dependent parameters were employed. The list of parameters and their uncertainties is similar to those listed for thorium, except fission parameters, as tungsten was assumed to be a non-fissile element. The threshold for fission is at about 60 MeV of neutron incident energy and was not included in the models. It was added subsequently as a dosimetry reaction in ENDF-6 File 10, since the cross section is so small that it contributes negligibly to the summation of the total cross section.

The definitions of cross sections in the cross-section parameter vector for all tungsten isotopes are given in Tables VIII-XII. Note that the energy grid is fixed and is the same for all reactions, but some reactions require fewer points due to their respective thresholds.

The covariance matrix prior was generated in the same way as for $^{232}$Th. In total, 449 files were produced for $^{180}$W, 498 for $^{182}$W, 499 for $^{183}$W, $^{184}$W and $^{186}$W. Relevant cross sections were extracted from the files, lumped reaction cross sections were constructed. The cross sections were packed into the cross-section parameter vector and the elements of the covariance matrix were generated as described for $^{232}$Th,

To account for additional unidentified uncertainties, the relative variance of all cross-section parameters was increased by 0.0009, which corresponds to 3 % standard deviation in the prior.

TABLE VIII: Cross-section definition in the parameter covariance vector of $^{180}$W in terms of the ENDF-6 reaction designation MT numbers. The `Npnt` column designates the number of energy points.

| Npnt | Contributing MTs |
|---|---|
| 74 | 2 (elastic) |
| 74 | $P_1(2)$ (first moment of the elastic) |
| 74 | $P_2(2)$ (second moment of the elastic) |
| 74 | $P_3(2)$ (third moment of the elastic) |
| 17 | 5 37 (lumped) |
| 14 | 16 41 (lumped) |
| 12 | 17 |
| 33 | 51 (first discrete inelastic) |
| 33 | $P_1(51)$ (first moment of 51) |
| 28 | 52 53 54 55 56 57 58 |
| 26 | 28 91 (lumped) |
| 74 | 102 |
| 20 | 600 601 602 603 604 605 606 607 608 609 610 611 612 613 614 649 (lumped) |
| 52 | 800 801 802 803 804 805 806 807 808 809 810 811 812 813 814 849 (lumped) |

TABLE IX: Cross-section definition in the parameter covariance vector of $^{182}$W in terms of the ENDF-6 reaction designation MT numbers. The `Npnt` column designates the number of energy points.

| Npnt | Contributing MTs |
|---|---|
| 74 | 2 |
| 74 | $P_1(2)$ (first moment of the elastic) |
| 74 | $P_2(2)$ (second moment of the elastic) |
| 74 | $P_3(2)$ (third moment of the elastic) |
| 16 | 5 37 (lumped) |
| 14 | 16 41 (lumped) |
| 12 | 17 |
| 33 | 51 (first discrete inelastic) |
| 33 | $P_1(51)$ (first moment of 51) |
| 28 | 52 53 54 55 56 57 58 59 (lumped) |
| 25 | 28 91 (lumped) |
| 74 | 102 |
| 19 | 600 601 602 603 604 605 606 607 608 609 610 611 612 613 614 615 616 617 618 619 620 621 622 623 624 625 626 627 628 629 649 (lumped) |
| 44 | 800 801 802 803 804 805 806 849 (lumped) |

### B. Selection of experimental data

#### *1. W-180*

No experimental data on $^{180}$W were available that could be used to improve the evaluation. The final file is identical to the prior.

The resonance parameters were formatted from the nu-

TABLE X: Cross-section definition in the parameter covariance vector of $^{183}$W in terms of the ENDF-6 reaction designation MT numbers. The `Npnt` column designates the number of energy points.

| Npnt | Contributing MTs |
|---|---|
| 74 | 2 |
| 74 | $P_1(2)$ (first moment of the elastic) |
| 74 | $P_2(2)$ (second moment of the elastic) |
| 74 | $P_3(2)$ (third moment of the elastic) |
| 17 | 5 37 (lumped) |
| 16 | 16 41 (lumped) |
| 12 | 17 |
| 35 | 51 (first discrete inelastic) |
| 35 | $P_1(51)$ (first moment of 51) |
| 34 | 52 53 54 55 56 57 58 59 60 (lumped) |
| | 61 |
| 27 | 28 91 (lumped) |
| 74 | 102 |
| 20 | 600 601 602 603 604 605 606 607 608 |
| | 609 610 611 612 613 614 649 (lumped) |
| 44 | 800 801 802 803 804 805 806 807 808 |
| | 809 810 811 812 813 814 815 816 817 |
| | 818 819 820 821 822 823 824 849 (lumped) |

TABLE XI: Cross-section definition in the parameter covariance vector of $^{184}$W in terms of the ENDF-6 reaction designation MT numbers. The `Npnt` column designates the number of energy points.

| Npnt | Contributing MTs |
|---|---|
| 74 | 2 |
| 74 | $P_1(2)$ (first moment of the elastic) |
| 74 | $P_2(2)$ (second moment of the elastic) |
| 74 | $P_3(2)$ (third moment of the elastic) |
| 16 | 5 37 (lumped) |
| 15 | 16 41 (lumped) |
| 12 | 17 |
| 33 | 51 (first discrete inelastic |
| 33 | $P_1(51)$ (first moment of 51) |
| 28 | 52 53 54 55 56 (lumped) |
| 25 | 28 91 (lumped) |
| 74 | 102 |
| 17 | 600 649 (lumped) |
| 29 | 800 801 802 803 804 805 806 807 849 (lumped) |

merical information in the Atlas of Resonance Parameters by S.F. Mughabghab [16]. No resonance covariances are given.

### *2. W-182*

The covariance matrix prior and the experimental data listed in Tables XIII-XIX were processed by the GANDR system. In the tables, the list includes all data found in the EXFOR database. Only the data sets with a "plus" sign in column-1 were included; those beginning with a "dash" were rejected.

TABLE XII: Cross-section definition in the parameter covariance vector of $^{186}$W in terms of the ENDF-6 reaction designation MT numbers. The `Npnt` column designates the number of energy points.

| Npnt | Contributing MTs |
|---|---|
| 74 | 2 |
| 74 | $P_1(2)$ (first moment of the elastic) |
| 74 | $P_2(2)$ (second moment of the elastic) |
| 74 | $P_3(2)$ (third moment of the elastic) |
| 20 | 5 37 (lumped) |
| 15 | 16 41 (lumped) |
| 12 | 17 |
| 33 | 51 (first discrete inelastic) |
| 33 | $P_1(51)$ (first moment of 51) |
| 27 | 52 53 54 55 56 57 58 59 60 |
| | 61 (lumped) |
| 25 | 28 91 (lumped) |
| 74 | 102 |
| 17 | 600 649 (lumped) |
| 22 | 800 849 (lumped) |

Fission cross-section measurements exist above 60 MeV, but the cross section is small. The nuclide was treated as non-fissile; the measured fission cross section was fitted by a polynomial and added as an activation reaction in File 10 with no assigned uncertainties.

Adjustment factors were applied to the cross sections and the data were formatted to create the final evaluated nuclear data file for $^{182}$W.

Resonance parameters were taken from JENDL-3.3 with small adjustments. The resonance covariances were prepared by the retro-active method [18] with the SAMMY code as follow:

- Retrieve best set of available resonance parameters.
- Convert the resonance parameters into the Reich-Moore form.
- Generate "experimental" cross sections for total, scattering, and capture cross sections with the NJOY code [49], for use as "experimental data" in SAMMY.
- Assign a global "experimental" uncertainty to the "experimental data." The uncertainties used were based on uncertainty in the thermal capture cross section and uncertainty in the capture resonance integrals.
- Run SAMMY code with the option to generate resonance-covariances retroactively.
- Convert the resonance-covariance results from SAMMY into the ENDF format for File 32 and MT=151.

TABLE XIII: Selection of total cross-section measurements of $^{182}$W from the EXFOR database.

| | EXFOR No. | Author | Year | Comment |
|---|---|---|---|---|
| + | 13887002 | F.S.Dietrich *et al.* | (03) | (42 points) |
| - | 22045008 | K.Knopf *et al.* | (87) | E=145 keV only |
| + | 11540009 | J.F.Whalen *et al.* | (82) | (272 points) Added 0.1 b statist. uncert. |
| - | 10803017 | P.T.Guenther *et al.* | (82) | |
| - | 40585034 | A.N.Djumin *et al.* | (77) | |
| + | 10047105 | D.G.Foster Jr *et al.* | (71) | (252 points) |
| - | 12159003 | R.C.Martin *et al.* | (67) | Old, scattered |
| - | 12168003 | W.Selove | (51) | Resonance reg. |

Systematic uncertainties:
3% for each EXFOR set
1% common to all measurements

TABLE XIV: Selection of radiative capture cross-section measurements of $^{182}$W from the EXFOR database.

| | Author | Year | EXFOR No. | Comment |
|---|---|---|---|---|
| - | J.Voignier *et al.* | (92) | 22006018 | repeated |
| - | K.Knopf *et al.* | (87) | 22045013 | Thermal |
| + | M.V.Bokhovko *et al.* | (86) | 40925003 | (32 points) Remove resonance data and data above inel. threshold |
| + | R.L.Macklin *et al.* | (83) | 10999006 | (32 points) Remove resonance data |
| - | S.Joly *et al.* | (81) | 21619012 | |
| - | Z.M.Bartolome *et al.* | (69) | 10002035 | Old, no uncert. |
| - | S.J.Friesenhahn | (66) | 12167011 | Low energy |
| - | S.J.Friesenhahn | (66) | 12167003 | Thermal |
| + | R.C.Block *et al.* | (66) | 11458006 | (4 points) Remove resonance data |
| - | S.V.Kapchigashev | (66) | 40755002 | Old, uncertain |
| - | V.N.Kononov *et al.* | (66) | 40076005 | No uncert. |
| - | H.Pomerance | (52) | 11507091 | Thermal |
| + | Artificial point at 1 MeV of 0.112±0.002 barns added for normalisation, based on integral benchmark considerations | | | |

Systematic uncertainties:
3% for each EXFOR set
3% common to all measurements

The resulting resonance parameters and covariances were used in the calculations of average cross sections and uncertainties. The calculations were done with SAMMY [39], NJOY [49], and PUFF-IV [51] codes. The results of these three codes agreed very well.

TABLE XV: Selection of elastic cross-section measurements of $^{182}$W from the EXFOR database.

| | Author | Year | EXFOR No. | Comment |
|---|---|---|---|---|
| + | P.T.Guenther *et al.* | (82) | 10803008 | |
| - | D.Lister *et al.* | (67) | 12174003 | No uncert. |

Systematic uncertainties:
10% for each EXFOR set

TABLE XVI: Selection of first discrete level inelastic cross-section measurements of $^{182}$W from the EXFOR database.

| | Author | Year | EXFOR No. | Comment |
|---|---|---|---|---|
| + | P.T.Guenther *et al.* | (82) | 10803014 | |
| + | D.Lister *et al.* | (67) | 12174004 | |

Systematic uncertainties:
10% for each EXFOR set
10% common to all measurements (altogether 14.1 %)

TABLE XVII: Selection of (n,2n+x) cross-section measurements of $^{182}$W from the EXFOR database.

| | Author | Year | EXFOR No. | Comment |
|---|---|---|---|---|
| + | Kong Xiangzhong | (97) | 31484005 | |
| + | J.Frehaut *et al.* | (80) | 20416050 | Corrected [52]; added uncert. 0.12% $^{252}$Cf $\overline{\nu}$ + 0.9% $^{238}$U(n,f) |
| + | S.M.Qaim *et al.* | (75) | 20668005 | |
| + | G.N.Maslov *et al.* | (72) | 40136019 | |
| + | W.Dilg *et al.* | (68) | 20802015 | |
| - | A.A.Druzhinin *et al.* | (66) | 40174002 | Outlier, no monitor x.s. |
| - | M.Lindner *et al.* | (59) | 12185004 | Outlier, old |

Systematic uncertainties:
1% for each EXFOR set
4% common to all measurements (altogether 4.1 %)

TABLE XVIII: Selection of (n,p) cross-section measurements of $^{182}$W from the EXFOR database.

| | Author | Year | EXFOR No. | Comment |
|---|---|---|---|---|
| + | V.Semkova *et al.* | (07) | 22877 | (4 points) |
| - | V.Avrigeanu *et al.* | (06) | 41469003 | = 41428045 |
| + | A.A.Filatenkov | (03) | 41428044 | (1 point) |
| + | A.A.Filatenkov | (03) | 41428045 | (6 points) |
| + | Kong Xiangzhong | (97) | 31484002 | (5 points) |
| + | A.Grallert *et al.* | (93) | 31496056 | |
| + | M.Lindner *et al.* | (59) | 12185003 | (1 point) |

Systematic uncertainties:
2% for each EXFOR set
10% common to all measurements

TABLE XIX: Selection of (n,$\alpha$) cross-section measurements from the EXFOR database.

| |
|---|
| Only data for isomer production are available and are not included in the fitting procedure. |

TABLE XX: Selection of total cross-section measurements of $^{183}$W from the EXFOR database.

| | Author | Year | EXFOR No. | Comment |
|---|---|---|---|---|
| + | K.Knopf *et al.* | (87) | 22045009 | E=143 keV point only |
| - | M.Ohkubo *et al.* | (78) | 20825002 | Resonance |
| + | M.Ohkubo[a] *et al.* | (78) | 20825 | Use broad bin averages at higher energies |
| - | W.Selove | (51) | 12168004 | Resonance |
| Systematic uncertainties: | | | | |
| 1% for each EXFOR set | | | | |
| 1% common to all measurements (altogether 2.8 %) | | | | |

### 3. *W-183*

The covariance matrix prior and the experimental data listed in Tables XX-XXVI were processed by the GANDR system. As before, the data sets with a dash in column-1 were rejected.

Fission cross-section measurements exist above 60 MeV, but the cross section is small. The nuclide was treated as non-fissile; the measured fission cross section was fitted by a polynomial and added as an activation reaction in File 10 with no assigned uncertainties.

Adjustment factors were applied to the cross sections and the data were formatted to create the final evaluated nuclear data file for $^{183}$W.

Resonance parameters were taken from JENDL-3.3 with small adjustments. The resonance covariances were prepared by the retro-active method [18] in the same way as for $^{182}$W.

TABLE XXI: Selection of (n,2n+x) cross-section measurements of $^{183}$W from the EXFOR database.

| | Author | Year | EXFOR No. | Comment |
|---|---|---|---|---|
| + | J.Frehaut *et al.* | (80) | 20416051 | Corrected [52]; added uncert. 0.12% $^{252}$Cf $\overline{\nu}$ + 0.9% $^{238}$U(n,f) |
| Systematic uncertainties: | | | | |
| 1% for each EXFOR set | | | | |

TABLE XXII: Selection of fission cross-section measurements of $^{183}$W from the EXFOR database.

| | Author | Year | EXFOR No. | Comment |
|---|---|---|---|---|
| - | V.P.Eismont *et al.* | (06) | 22937 | Not fitted. |

TABLE XXIII: Selection of (n,n+p) cross-section measurements of $^{183}$W from the EXFOR database.

| | Author | Year | EXFOR No. | Comment |
|---|---|---|---|---|
| - | V.Semkova *et al.* | (07) | 22877 | Not fitted |

TABLE XXIV: Selection of the first discrete level inelastic cross-section measurements of $^{183}$W from the EXFOR database.

| | Author | Year | EXFOR No. | Comment |
|---|---|---|---|---|
| - | B.Anders,et.al. | (82) | 21818007 | Metastable isomer product. (not fitted) |

TABLE XXV: Selection of radiative capture cross-section measurements of $^{183}$W from the EXFOR database.

| | Author | Year | EXFOR No. | Comment |
|---|---|---|---|---|
| - | J.Voignier *et al.* | (92) | 22006 | Equal to 10 |
| - | K.Knopf *et al.* | (87) | 22045 | Thermal |
| + | M.V.Bokhovko *et al.* | (86) | 40925004 | Removed data above inelastic threshold |
| - | R.L.Macklin *et al.* | (83) | 10999 | (34 points) |
| - | S.Joly *et al.* | (81) | 21619 | (3 points) |
| - | Grenier *et al.* | (81) | - | (3 points) |
| - | S.J.Friesenhahn | (66) | 12167 | Low energy (32 points) |
| - | S.J.Friesenhahn | (66) | 12167 | Thermal |
| + | R.C.Block *et al.* | (66) | 11458009 | Removed resonance data |
| - | S.V.Kapchigashev | (66) | 40755 | Low energies with no uncert. removed |
| + | V.N.Kononov *et al.* | (66) | 40076 | (5 points) |
| - | Z.M.Bartolome *et al.* | (69) | 10002 | raw data |
| - | H.Pomerance | (52) | 11507 | Thermal |
| Systematic uncertainties: | | | | |
| 1 % for each EXFOR set | | | | |
| 3 % common to all measurements | | | | |

TABLE XXVI: Selection of (n,$\alpha$) cross-section measurements of $^{183}$W from the EXFOR database.

| |
|---|
| Only data for isomer production given; no data fitted. |

TABLE XXVII: Selection of (n,p) cross-section measurements of $^{183}$W from the EXFOR database.

| | Author | Year | EXFOR No. | Comment |
|---|---|---|---|---|
| + | V.Semkova *et al.* | (07) | 22877 | |
| - | V.Avrigeanu *et al.* | (06) | 41469006 | =41428009 |
| + | A.A.Filatenkov | (03) | 41428009 | |
| + | A.Grallert *et al.* | (93) | 31496057 | |
| + | S.M.Qaim *et al.* | (75) | 20668009 | |
| + | M.Lindner *et al.* | (59) | 12185005 | |

Systematic uncertainties:
Added covariance of each measurement equals minimum variance of the same.
10 % common to all measurements

TABLE XXVIII: Selection of total cross-section measurements of $^{184}$W from the EXFOR database.

| | Author | Year | EXFOR No. | Comment |
|---|---|---|---|---|
| + | F.S.Dietrich *et al.* | (03) | 13887003 | |
| + | Bessheyoko *et al.* | (92) | - | |
| + | K.Knopf *et al.* | (87) | 22045010 | Only 143 keV |
| - | V.A.Anufriev *et al.* | (83) | 40850004 | Resonance |
| - | J.A.Harvey *et al.* | (82) | 12897005 | Resonance |
| + | J.F.Whalen *et al.* | (82) | 11540019 | Resonance |
| + | P.T.Guenther *et al.* | (82) | 10803018 | |
| + | A.N.Djumin *et al.* | (77) | 40585035 | |
| + | D.G.Foster Jr *et al.* | (71) | 10047106 | |
| - | R.C.Martin *et al.* | (67) | 12159004 | Old |

Systematic uncertainties:
3% for each EXFOR set
1% common to all measurements (altogether 2.8 %)

### *4. W-184*

The covariance matrix prior and the experimental data listed in Tables XXVIII-XXXIX were processed by the GANDR system. As before, the data sets with a dash in column-1 were rejected.

Fission cross section measurements exist above 60 MeV, but the cross section is small. The nuclide was treated as non-fissile; the measured fission cross section was fitted by a polynomial and added as an activation reaction in File 10 with no assigned uncertainties.

Adjustment factors were applied to the cross sections and the data were formatted to create the final evaluated nuclear data file for $^{184}$W.

Resonance parameters were taken from JENDL-3.3 with small adjustments. The resonance covariances were prepared by the retro-active method [18] in the same way as for $^{182}$W. In the unresolved resonance range a 5 % systematic uncertainty was added to capture.

TABLE XXIX: Selection of elastic cross-section measurements of $^{184}$W from the EXFOR database.

| | Author | Year | EXFOR No. | Comment |
|---|---|---|---|---|
| - | V.A.Anufriev *et al.* | (83) | 40850007 | Thermal (1point) |
| + | P.T.Guenther *et al.* | (82) | 10803009 | (13 points) |
| - | D.Lister *et al.* | (67) | 12174006 | No uncert. |

Systematic uncertainties:
10% for each EXFOR set

TABLE XXX: Selection of (n,2n+x) cross-section measurements of $^{184}$W from the EXFOR database.

| | Author | Year | EXFOR No. | Comment |
|---|---|---|---|---|
| + | Frehaut *et al.* | (80) | 20416052 | Corrected [52]; added uncert. 0.12% $^{252}$Cf $\overline{\nu}$ + 0.9% $^{238}$U(n,f) |

Systematic uncertainties:
1% for each EXFOR set

### *5. W-186*

The covariance matrix prior and the experimental data listed in Tables XL-XLVI were processed by the GANDR system. As before, the data sets with a dash in column-1 were rejected.

Fission cross section measurements exist above 60 MeV, but the cross section is small. The nuclide was treated as non-fissile; the measured fission cross section was fitted by a polynomial and added as an activation reaction in File 10 with no assigned uncertainties.

Adjustment factors were applied to the cross sections and the data were formatted to create the final evaluated nuclear data file for $^{186}$W.

Resonance parameters were taken from IRDF-2002 with small adjustments. The resonance covariances were prepared by the retro-active method [18] in the same way as for $^{182}$W.

TABLE XXXI: Selection of $^{184}$W(n,2n)$^{183m}$W cross-section measurements from the EXFOR database.

| Author | Year | EXFOR No. | Comment |
|---|---|---|---|
| - B.Anders *et al.* | (82) | 21818008 | Cannot be processed |
| - R.Prasad *et al.* | (66) | 30015008 | Cannot be processed |

TABLE XXXII: Selection of (n,3n+x) cross-section measurements of $^{184}$W from the EXFOR database (not fitted).

| Author | Year | EXFOR No. | Comment |
|---|---|---|---|
| - J.Frehaut *et al.* | (80) | 20416060 | Corrected [52]; added uncert. 0.12% $^{252}$Cf $\overline{\nu}$ + 0.9% $^{238}$U(n,f) |

TABLE XXXIII: Selection of fission cross-section measurements of $^{184}$W from the EXFOR database.

| Author | Year | EXFOR No. | Comment |
|---|---|---|---|
| - V.P.Eismont *et al.* | (06) | 22937004 | Not fitted |

TABLE XXXV: Selection of first discrete level inelastic cross-section measurements of $^{184}$W from the EXFOR database.

| | Author | Year | EXFOR No. | Comment |
|---|---|---|---|---|
| + | P.T.Guenther *et al.* | (82) | 10803015 | |
| + | D.Lister *et al.* | (67) | 12174007 | |

Systematic uncertainties:
10% for each EXFOR set
10% common to all measurements (altogether 14.1 %)

TABLE XXXIV: Selection of (n,n+p) cross-section measurements of $^{184}$W from the EXFOR database.

| Author | Year | EXFOR No. | Comment |
|---|---|---|---|
| - V.Semkova *et al.* | (07) | 22877 | |
| - H.Sakane *et al.* | (03) | 22827018 | |
| - S.M.Qaim *et al.* | (75) | 20668012 | |
| - A.K.Ganguly *et al.* | (63) | 31329005 | |

TABLE XXXVI: Selection of radiative capture cross-section measurements of $^{184}$W from the EXFOR database.

| | Author | Year | EXFOR No. | Comment |
|---|---|---|---|---|
| - | V.Bondarenko *et al.* | (05) | 31572004 | Thermal |
| - | J.Voignier *et al.* | (92) | 22006020 | |
| - | K.Knopf *et al.* | (87) | 22045015 | Thermal |
| + | M.V.Bokhovko *et al.* | (86) | 40925005 | |
| - | V.A.Anufriev *et al.* | (83) | 40850008 | Thermal |
| + | R.L.Macklin *et al.* | (83) | 10999008 | |
| - | H.Beer *et al.* | (81) | 21768002 | |
| - | H.Beer *et al.* | (81) | 21768003 | |
| - | S.Joly *et al.* | (81) | 21619014 | |
| - | S.J.Friesenhahn | (66) | 12167006 | Low energy |
| + | R.C.Block *et al.* | (66) | 11458007 | |
| - | S.V.Kapchigashev | (66) | 40755004 | |
| - | S.J.Friesenhahn | (66) | 12167007 | Thermal |
| - | Z.M.Bartolome *et al.* | (69) | 10002039 | |
| - | V.N.Kononov *et al.* | (66) | 40076006 | No uncert. |
| - | R.Booth *et al.* | (58) | 11429027 | |
| - | H.Pomerance | (52) | 11507093 | Thermal |

Systematic uncertainties:
1% for each EXFOR set
10% common to all measurements

TABLE XXXVII: Selection of $^{184}$W(n,$\gamma$)$^{185m}$W cross-section measurements from the EXFOR database.

| Author | Year | EXFOR No. | Comment |
|---|---|---|---|
| - S.K.Mangal *et al.* | (62) | 31248015 | Cannot be processed |

TABLE XXXVIII: Selection of (n,p) cross-section measurements of $^{184}$W from the EXFOR database.

| | Author | Year | EXFOR No. | Comment |
|---|---|---|---|---|
| + | V.Semkova *et al.* | (07) | 22877 | |
| - | V.Avrigeanu *et al.* | (06) | 41469008 | =41428011 |
| + | R.Eichin *et al.* | (05) | | |
| + | A.A.Filatenkov | (03) | 41428011 | |
| + | A.A.Filatenkov | (99) | 41298091 | |
| + | A.A.Filatenkov | (99) | 41240105 | |
| + | Kong Xiangzhong | (97) | 31484003 | |
| + | Y.Kasugai *et al.* | (94) | 22351007 | |
| + | A.Grallert *et al.* | (93) | 31496058 | |
| + | Y.Ikeda *et al.* | (88) | 22089107 | |
| + | S.M.Qaim *et al.* | (75) | 20668012 | Corrected |
| + | S.K.Mukherjee *et al.* | (63) | 31330010 | |
| - | A.Poularikas *et al.* | (60) | 12181002 | Old |
| - | R.F.Coleman *et al.* | (59) | 21440024 | Old |

Systematic uncertainties:
2% for each EXFOR set
10% common to all measurements

TABLE XXXIX: Selection of (n,$\alpha$) cross-section measurements of $^{184}$W from the EXFOR database.

| | Author | Year | EXFOR No. | Comment |
|---|---|---|---|---|
| + | V.Semkova *et al.* | (07) | 22877 | |
| - | V.Avrigeanu *et al.* | (06) | 41469009 | =41428010 |
| + | R.Eichin *et al.* | (05) | | |
| + | A.A.Filatenkov | (03) | 41428010 | |
| + | Y.Kasugai *et al.* | (94) | 23011004 | =22351009 |
| + | A.Grallert *et al.* | (93) | 31496028 | |
| - | Y.Kasugai *et al.* | (92) | 22351009 | |
| + | S.M.Qaim *et al.* [r] | (75) | 20668014 | Corrected |
| + | M.Lindner *et al.* | (59) | 12185006 | |

Systematic uncertainties:
2% for each EXFOR set
3% common to all measurements

TABLE XL: Selection of total cross-section measurements of $^{186}$W from the EXFOR database.

| | Author | Year | EXFOR No. | Comment |
|---|---|---|---|---|
| + | F.S.Dietrich *et al.* | (03) | 13887 | |
| + | K.Knopf *et al.* | (87) | 22045 | Only 143 keV |
| + | J.F.Whalen *et al.* | (82) | 11540 | Add 0.1 b uncertainty |
| + | P.T.Guenther *et al.* | (82) | 10803 | |
| + | D.G.Foster Jr *et al.* | (71) | 10047 | |
| - | A.N.Djumin *et al.* | (77) | 40585 | Single point |
| - | R.C.Martin *et al.* | (67) | 12159 | Old |
| - | W.Selove | (51) | 12168 | Old |

Systematic uncertainties:
2% for each EXFOR set
2% common to all measurements

### C. Analysis of obtained covariances

The full evaluated files with covariances were verified by the ENDF Utility Codes [48] to check for the formal correctness. In the next step the covariance plots were generated on a fine energy grid with the NJOY processing system [49] to check processability and the general features of the covariance matrices, including cross-reaction correlations. An example of the cross-correlation matrix between the $^{183}$W elastic and inelastic cross sections is shown in Figure 6. Swings of the correlation pattern from strong anti-correlations around 1 MeV to strong correlations around 4-5 MeV are observed. Similarly, the cross-correlation matrix between the $^{183}$W first-discrete-level inelastic and (n,2n) cross sections is shown in Figure 7. In this particular case the (n,2n) reaction is included in the lumped reaction designated MT=852, but since the threshold of the (n,2n+p) reaction is 14.71 MeV, the matrix corresponds purely to the (n,2n) reaction below this energy. At higher energies some approximation is needed to obtain the uncertainty of the pure (n,2n) cross section, but in this energy range the (n,2n) cross section is decreasing rapidly to a small value and its uncertainty is usually less important. Note the relatively strong and uniform anti-correlation between the inelastic and the (n,2n) reactions, as expected for the dominant channels in the given energy range, arising from the physics constraint that the total cross section equals to the sum of the partials. An example of the correlation matrix for the capture reaction of $^{186}$W is shown in Figure 8. Additional plots of the covariance matrices for the capture reaction of $^{186}$W in the fast neutron region were generated online at the IAEA website (see Figures 1, 2 and 3 in previous section).

Broad-group testing of the calculated covariances was

TABLE XLI: Selection of (n,2n+x) cross-section measurements of $^{186}$W from the EXFOR database.

| | Author | Year | EXFOR No. | Comment |
|---|---|---|---|---|
| + | A.A.Filatenkov | (03) | 41428012 | (5 points) |
| + | Kong Xiangshong | (97) | 31484006 | (5 points) |
| + | J.Frehaut *et al.* | (80) | 20416053 | Corrected [52]; added uncert. 0.12% $^{252}$Cf $\overline{\nu}$ + 0.9% $^{238}$U(n,f) |
| - | A.A.Druzhinin *et al.* | (66) | 40174061 | Old |
| - | M.Lindner | (59) | 12185007 | Old |

Systematic uncertainties:
1% systematic for each data set.
4% common to all measurements

TABLE XLII: Selection of (n,3n+x) cross-section measurements of $^{186}$W from the EXFOR database.

| | Author | Year | EXFOR No. | Comment |
|---|---|---|---|---|
| + | J.Frehaut *et al.* | (80) | 20416061 | Corrected [52]; added uncert. 0.12% $^{252}$Cf $\overline{\nu}$ + 0.9% $^{238}$U(n,f) |

Systematic uncertainties:
1% for each EXFOR set
4% common to all measurements

TABLE XLIII: Selection of first discrete level inelastic cross-section measurements of $^{186}$W from the EXFOR database.

| | Author | Year | EXFOR No. | Comment |
|---|---|---|---|---|
| + | D.Lister *et al.* | (67) | 12174 | (59 points) |
| + | P.T.Guenther *et al.* | (82) | 10803 | (15 points) |

Systematic uncertainties:
10% for each EXFOR set
10% common to all measurements (altogether 2.8 %)

TABLE XLIV: Selection of radiative capture cross-section measurements of $^{186}$W from the EXFOR database.

| | Author | Year | EXFOR No. | Comment |
|---|---|---|---|---|
| + | G.D.Kim *et al.* | (07) | 20673035 | (3 points) |
| - | M.Karadag *et al.* | (04) | 22842002 | Thermal |
| - | Vuong Huu Tan *et al.* | (04) | 31542002 | |
| - | Guohui Zhang *et al.* | (01) | 32550002 | |
| - | J.Voignier *et al.* | (92) | 22006021 | |
| - | K.Knopf *et al.* | (87) | 22045016 | Thermal |
| + | Yu.N.Trofimov | (87) | 41001037 | (1 point) |
| + | M.V.Bokhovko *et al.* | (86) | 40925006 | (19 points) $>$ 50 keV |
| - | M.V.Bokhovko *et al.* | (86) | 40925006 | (38 points) $>$ 50 keV |
| + | R.L.Macklin *et al.* | (83) | 10999009 | (34 points) |
| + | S.Joly *et al.* | (81) | 21619015 | (3 points) |
| - | V.A.Anufriev *et al.* | (81) | 40608003 | Thermal |
| + | G.Magnusson *et al.* | (80) | 21004004 | (1 point) |
| - | T.Bradley *et al.* | (79) | 10938006 | |
| - | G.Gleason | (77) | 10662014 | Thermal |
| - | M.Lindner *et al.* | (76) | 10221044 | |
| - | O.Schwerer *et al.* | (76) | 20670016 | |
| + | M.Valkonen | (76) | 20673035 | (1 point) |
| - | K.Siddappa *et al.* | (74) | 30502018 | |
| - | C.H.Hogg *et al.* | (70) | 12602007 | Thermal |
| - | M.Diksic *et al.* | (70) | 30023012 | |
| - | Z.M.Bartolome *et al.* | (69) | 10002041 | |
| - | G.G.Zaikin *et al.* | (68) | 40248004 | |
| - | P.P.Damle *et al.* | (67) | 20184002 | Thermal |
| - | V.N.Kononov *et al.* | (66) | 40076007 | |
| - | S.J.Friesenhahn | (66) | 12167009 | Thermal |
| - | S.J.Friesenhann | (66) | 12167008 | Resonance |
| - | S.V.Kapchigashev | (66) | 40755005 | Resonance |
| + | R.C.Block *et al.* | (66) | 11458008 | (9 points) |
| - | A.K.Chaubey *et al.* | (65) | 30079035 | |
| - | J.A.Miskel *et al.* | (62) | 12115005 | |
| - | J.A.Miskel *et al.* | (62) | 12115006 | |
| - | W.S.Lyon | (60) | 11625032 | Thermal |
| - | Yu.Ya.Stavisskii | (60) | 40452005 | |
| - | A.E.Johnsrud *et al.* | (59) | 11675025 | |
| - | W.S.Lyon *et al.* | (59) | 11407030 | |
| - | R.Booth *et al.* | (58) | 11429028 | |
| - | A.I.Leipunskij | (58) | 40244036 | |
| - | V.N.Kononov *et al.* | (58) | 40421023 | |
| - | M.V.Pasechnik *et al.* | (58) | 40336093 | |
| - | A.I.Leipunskij | (58) | 40244017 | |
| - | A.I.Leipunskij | (58) | 40244058 | |
| - | J.L.Perkin *et al.* | (58) | 21438025 | |
| - | R.L.Macklin *et al.* | (57) | 11399045 | (1 point) |
| - | H.Pomerance | (52) | 11507094 | Thermal |
| - | L.E.Beghian *et al.* | (49) | 22580014 | |
| - | L.Seren *et al.* | (47) | 11447115 | Thermal |

Systematic uncertainties:
3% for each EXFOR set
1% common to all measurements

TABLE XLV: Selection of (n,p) cross-section measurements of $^{186}$W from the EXFOR database.

| | Author | Year | EXFOR No. | Comment |
|---|---|---|---|---|
| + | V.Semkova *et al.* | (07) | 22877 | (3 points) |
| + | A.A.Filatenkov *et al.* | (03) | 41428014 | (7 points) |
| + | A.A.Filatenkov *et al.* | (99) | 41240106 | (8 points) |
| + | Y.Satoh *et al.* | | 22365012 | (5 points) |
| + | A.A.Filatenkov *et al.* | (99) | 41298012 | (1 point) |
| + | S.Murahira *et al.* | (95) | 22311014 | (6 points) |
| + | Y.Kasugai *et al.* | (92) | 22351008 | (5 points) |
| + | S.M.Qaim *et al.* | (75) | 20668017 | (1 point) |
| - | S.K.Mukherjee *et al.* | (63) | 31330012 | (1 point) |
| - | A.Poularikas *et al.* | (60) | 12181004 | (1 point) |
| - | R.F.Coleman *et al.* | (59) | 21440025 | (1 point) |

Systematic uncertainties:
2% for each EXFOR set
10% common to all measurements

TABLE XLVI: Selection of (n,$\alpha$) cross-section measurements of $^{186}$W from the EXFOR database.

| | Author | Year | EXFOR No. | Comment |
|---|---|---|---|---|
| + | V.Semkova *et al.* | (07) | 22877 | (6 points) |
| + | A.A.Filatenkov *et al.* | (03) | 41428013 | (7 points) |
| + | Kong Xiangzhong | (97) | 31484004 | (5 points) |
| + | A.Grallert *et al.* | (93) | 31496029 | (1 point) |
| + | Y.Kasugai *et al.* | (92) | 22351010 | (6 points) |
| + | Y.Ikeda *et al.* | (88) | 22089108 | (4 points) |
| + | S.M.Qaim *et al.* | (75) | 20668019 | (1 point) |
| - | S.K.Mukherjee *et al.* | (63) | 31330011 | (1 point) |
| - | A.Poularikas *et al.* | (60) | 12181003 | (1 point) |

Systematic uncertainties:
1% for each EXFOR set
5% common to all measurements

performed by calculating the thermal cross sections and the resonance integrals with their respective uncertainties. The values are given in Table XLVII. The capture reaction of $^{186}$W is the only one that can be measured by the activation technique because the intensities of the gamma rays from the activation of $^{184}$W are low. The thermal cross section and the resonance integral are about 10 % higher than the values derived from the activation analysis constants recommended by IUPAC [50], but the absolute $\gamma$-emission probabilities are difficult to measure. The recommended value of $\gamma$-emission probabilities in ENSDF database has changed in recent years by as much as 20 %.

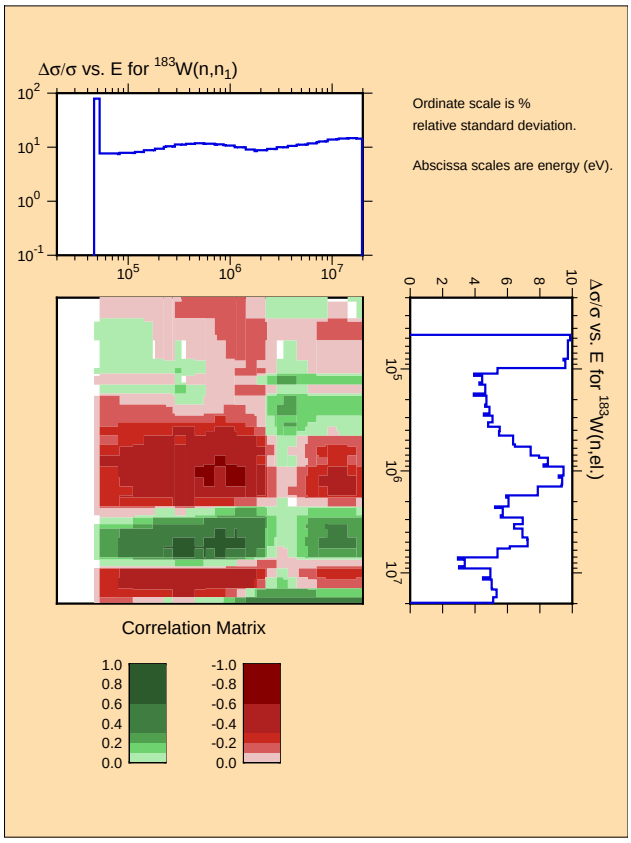


FIG. 6: Uncertainties and cross-correlation matrix of the $^{183}$W elastic and first-discrete-level inelastic cross sections.

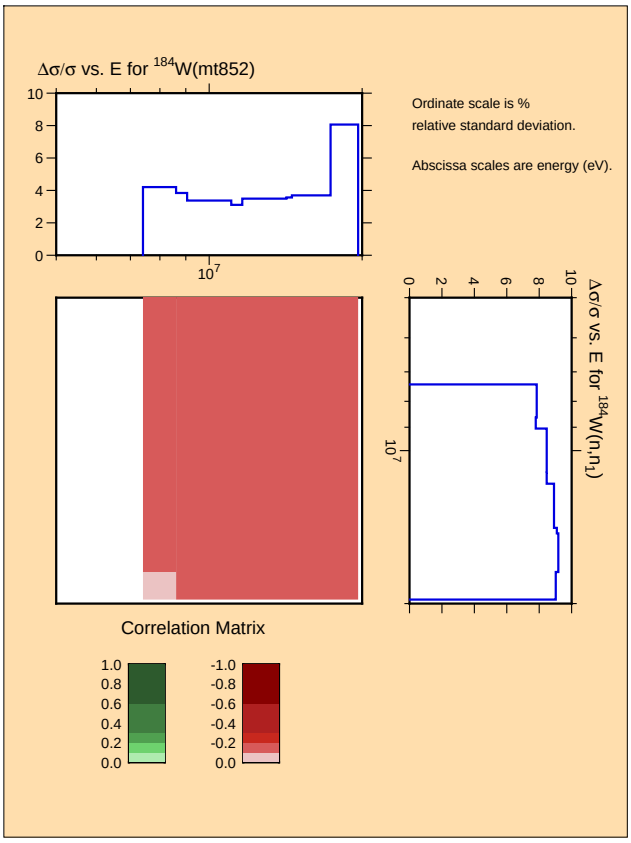


FIG. 7: Uncertainties and cross-correlation matrix of the $^{184}$W first-discrete-level inelastic and (n,2n) cross sections.

## V. EVALUATION OF MANGANESE

### A. EMPIRE model calculations

As in the case of the $^{232}$Th evaluation, the details of the selection of optical model and other parameters are described in a separate paper [21]. The list of parameters and their uncertainties is similar to those parameters used in thorium (fission parameters are obviously not required for manganese).

The definitions of cross sections in the cross-section parameter vector for manganese are given in Table XLVIII. Note that the energy grid is fixed and is the same for all reactions, but some reactions require fewer points due to their respective thresholds.

### B. Selection of experimental data

In the fast energy range the experimental data for radiative capture show significant discrepancies, comparable to the uncertainty of the prior. Preliminary analysis of integral experiments is also to some extent contradictory. For other reaction channels - except perhaps the (n,2n) reaction - the experimental data would not have a significant impact on the covariances, therefore the final covariance matrix in the fast energy range is equal to the prior. Note that a new comprehensive evaluation of the $^{55}$Mn(n,2n) reaction for reactor dosimetry has been undertaken by Zolotarev, including a careful assesment of available experimental data [53]. The new dosimetry evaluation has smaller uncertainties, but the cross sections are in good agreement at least in the plateau region. Slight differences are observed near threshold, but they are within the assigned uncertainties.

The resonance parameters were obtained from a sequential Bayes SAMMY analysis of the most recent experimental neutron transmissions and capture cross sections in the resolved energy range (1.0-5 eV to 125 keV): Harvey *et al.* transmissions measured at ORELA in 1980 [54], Aerts *et al.* capture cross sections measured at GELINA in 2006 [55], and Guber *et al.* capture cross section measured at ORELA in 2007 [56]. For the evaluation in the thermal energy range, Widder*et al.* (1975) capture cross section [57], Coté *et al.* (1964) total cross sections [58], and Rainwater *et al.* (1947) total cross sections [59] were considered. The thermal capture cross sections were normalized at the 0.0253 eV value of 13.27 b which is an average of the available experimental values.

The uncertainties and covariances of the resonance parameters in File 32 were generated only from the statistical uncertainties of the experimental database.

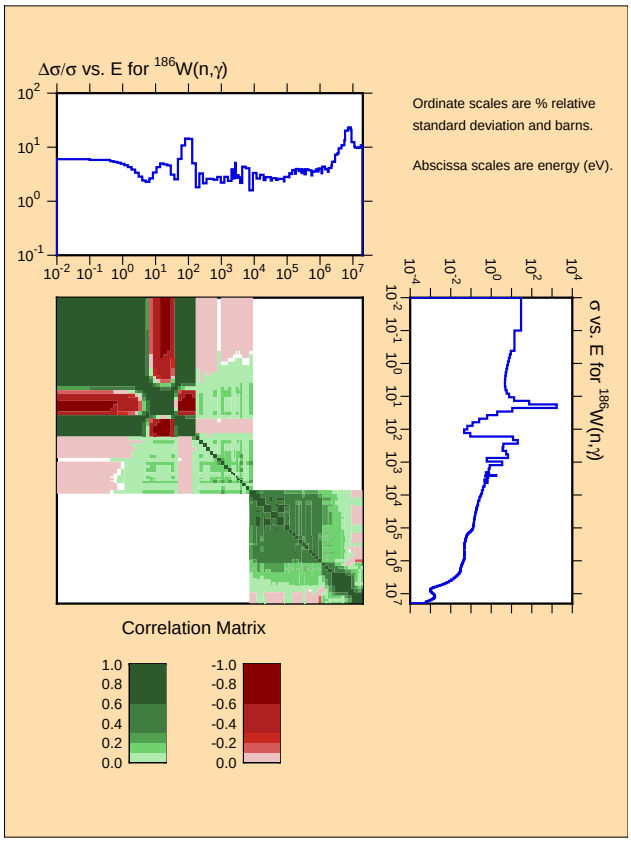


FIG. 8: Uncertainty and correlation matrix of the $^{186}$W(n,$\gamma$) reaction.

The systematic uncertainties were estimated from results obtained in the SAMMY analysis of the experimental database, from some information found in the publications, and from discussion with some authors. These uncertainties were included as additional uncertainty in File 33 for the total, elastic and radiative capture cross-section covariances, and are to be combined with the cross-section uncertainties obtained from the resonance parameters stored in File 32 to obtain the corresponding total uncertainties.

### C. Analysis of obtained covariances

The full evaluated files with covariances were verified with the ENDF Utility Codes [48] to check for the formal correctness. In the next step the covariance plots were generated on a fine energy grid with the NJOY processing system [49] to check processability and the general features of the covariance matrices, including cross-reaction correlations. No problems were identified. An example of the covariance matrix for the capture reaction up to 60 MeV is shown in Figure 9. The uncertainty (variance) is higher near 10 MeV, where the cross section has a dip (and experimental data are not available), and at higher energies where the cross section becomes very small.

TABLE XLVII: Thermal cross sections and resonance integrals with uncertainties of the tungsten isotopes.

| Reaction | $\sigma_0$ [b] | RI [b] |
|---|---|---|
| $^{180}$W(n,tot) | 39.61 ± 26 % | 537.9 ± 7.2 % |
| $^{180}$W(n,el) | 9.96 ± 36 % | 284.6 ± 13.4 % |
| $^{180}$W(n,$\gamma$) | 29.65 ± 33 % | 249.6 ± 4.8 % |
| $^{182}$W(n,tot) | 29.55 ± 3.0 % | 1124. ± 2.9 % |
| $^{182}$W(n,el) | 8.84 ± 6.3 % | 492. ± 5.5 % |
| $^{182}$W(n,$\gamma$) | 20.71 ± 3.5 % | 628. ± 2.7 % |
| $^{183}$W(n,tot) | 12.49 ± 4.6 % | 822.8 ± 5.0 % |
| $^{183}$W(n,el) | 2.38 ± 8.1 % | 478.5 ± 7.8 % |
| $^{183}$W(n,$\gamma$) | 10.11 ± 5.5 % | 338.9 ± 5.0 % |
| $^{184}$W(n,tot) | 8.854 ± 2.9 % | 331.1 ± 2.0 % |
| $^{184}$W(n,el) | 7.353 ± 3.2 % | 311.2 ± 2.1 % |
| $^{184}$W(n,$\gamma$) | 1.501 ± 9.4 % | 15.6 ± 5.6 % |
| $^{186}$W(n,tot) | 38.17 ± 5.9 % | 3645. ± 2.2 % |
| $^{186}$W(n,el) | .0852 ± 100 % | 3158. ± 2.8 % |
| $^{186}$W(n,$\gamma$) | 38.08 ± 5.9 % | 483. ± 4.4 % |

The thermal capture cross section and the resonance integral are shown in Table XLIX. They are in excellent agreement with the values derived from the activation analysis constants recommended by IUPAC [50]. The uncertainty in the thermal cross section derived from the neutron activation constants seems low. We consider the assigned uncertainty in the evaluated cross sections file to be reasonable.

## VI. SUMMARY AND CONCLUSIONS

A self-consistent method of generating covariance information that combines the theoretical and experimental uncertainties was developed and first applied in the evaluation of $^{232}$Th within an IAEA coordinated research project. It includes medium and long-range correlations (in terms of energy) and correlations between different reaction channels that originate from physics constraints in the nuclear reaction models. These correlations are introduced through the covariance matrix prior calculated by a Monte Carlo method based on the EMPIRE code that implements the nuclear reaction modelling. In this way the physical consistency of the cross sections is preserved even after a subsequent least-squares adjustment. Small adjustments to the cross sections are calculated by the introduction of experimental data using the generalised least-squares method as implemented in the GANDR code. The main function of the fitting is to produce the evaluated mean values consistent with produced covariances, and to constrain the covariances based on accurate experimental data. Using statistically consistent (non-discrepant) experimental data is of primary importance. Failure to correctly account for correlations between experiments or to underestimate the systematic

TABLE XLVIII: Cross-section definition in the parameter covariance vector of $^{55}$Mn in terms of the ENDF-6 reaction designation MT numbers. The `Npnt` column designates the number of energy points.

| Npnt | | Contributing MTs |
|---|---|---|
| 74 | 2 | (elastic) |
| 74 | $P_1(2)$ | (first moment of the elastic) |
| 74 | $P_2(2)$ | (second moment of the elastic) |
| 74 | $P_3(2)$ | (third moment of the elastic) |
| 17 | 5 | 37 (lumped) |
| 13 | 16 | |
| 11 | 17 | |
| 32 | 51 | (first discrete inelastic) |
| 32 | $P_1(51)$ | (first moment of 51) |
| 23 | 52 | 53 54 55 56 57 58 59 60 |
| 20 | 61 | 62 63 64 65 66 67 68 69 |
| | 70 | (lumped) |
| 19 | 71 | 72 73 74 75 76 77 78 79 |
| | 80 | 81 82 83 84 85 86 87 88 |
| | 89 | 91 (lumped) |
| 74 | 102 | |
| 19 | 600 | 601 602 603 604 605 606 607 608 |
| | 609 | 610 611 612 613 614 615 616 617 |
| | 618 | 619 620 621 622 623 624 625 626 |
| | 627 | 628 629 630 631 632 649 (lumped) |
| 19 | 800 | 801 802 803 804 805 806 807 808 |
| | 809 | 810 811 812 813 814 815 816 817 |
| | 818 | 819 820 821 822 823 824 825 826 |
| | 827 | 828 829 830 831 (lumped) |

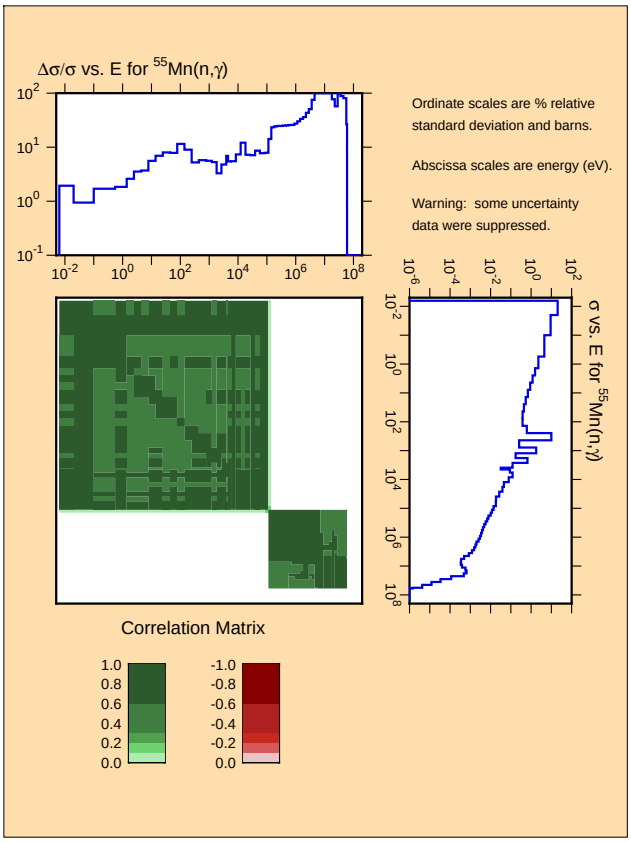


FIG. 9: Uncertainty and correlation matrix of the $^{55}$Mn(n,$\gamma$) reaction.

TABLE XLIX: Comparison of thermal capture cross section and resonance integral uncertainties of $^{55}$Mn with values derived from constants for neutron activation analysis [50].

| | IUPAC/Nudat | | ENDF/B-VII.1 | | |
|---|---|---|---|---|---|
| | | Uncert. | | Uncert. | Difference |
| | [barns] | [%] | [barns] | [%] | [%] |
| $\sigma_0$ | 13.19 | 0.6 | 13.27 | 1.1 | 0.7 |
| RI | 13.9 | 3.1 | 13.26 | 3.8 | -0.5 |

uncertainties may lead to unrealistically small uncertainties in resulting calculations.

An extra bonus of the developed methodology is that new (independent) experimental data (both differential and integral) can be introduced to further improve the cross sections and constrain the uncertainties in the future, as customary in Bayesian approaches. Improvements in one reaction channel will be correctly propagated to all other channels through correlations, including the total cross section. The price to pay is that all cross section covariances are given on the same energy grid and that in some cases several reactions are lumped together. This may be inconvenient for users, who are specifically interested in a particular reaction channel, but is well suited for applications in deterministic neutron transport.

Developed methodology has been applied to obtain high-quality nuclear data evaluations that include covariances for $^{232}$Th, $^{180,182,183,184,186}$W and $^{55}$Mn nuclei. These evaluated nuclear data files will be included into the ENDF/B-VII.1 library release.

## ACKNOWLEDGEMENTS

The IAEA is grateful to all participant laboratories for their assistance in the work and for support of the Coordinated Research Project (CRP) meetings and activities. The work described in this paper would not have been possible without IAEA Member States contributions.

The work was supported by the IAEA CRP on "Evaluated Nuclear Data Files for the Th-U Fuel Cycle", the IAEA Data Development Project on the "Maintenance and Upgrading of the International Reactor Dosimetry library (IRDF)", the EFDA (Project TW6-TTMN-001B task D7b), and by the Slovenian Research Agency (Reactor Physics Programme Group).

The authors would like to acknowledge the very important contribution made to the whole project by the EMPIRE development team lead by coordinator M.W. Her-

man.

We are especially grateful to P. Obložinský and D.L. Smith for their encouragement, advice and continued support of the covariance developments.

We would like to thank V. Zerkin who is involved in the development of visualization and dissemination tools to deal with covariance data that play a crucial role in described evaluation process.

[1] S.M. Bowman, "SCALE 6: Comprehensive Nuclear Safety Analysis Code System ", Nucl. Technol. **174**, 126-148, May 2011.

[2] I. Kodeli, "Multidimensional Deterministic Nuclear Data Sensitivity and Uncertainty Code System: Method and Application ", Nucl. Sci. & Eng. **138**, 45-66 (2001)

[3] "Covariance matrix evaluation and processing in the resolved/unresolved resonance regions ", Final report of the *NEA/WPEC-20*, ISBN 92-64-02302-X, Coordinator T. Kawano, WPEC, Nuclear Energy Agency, OECD 2008, Paris, France, .

[4] "Covariance Data in the Fast Neutron Region", Final report of the *NEA/WPEC-24*, NEA/NSC/WPEC/DOC(2010)427, Coordinator M. Herman, WPEC, Nuclear Energy Agency, OECD 2011, Paris, France.

[5] "Uncertainty and target accuracy assessment for innovative systems using recent covariance data evaluations", Final report of the *NEA/WPEC-26*, ISBN 978-92-64-99053-1, Coordinator M. Salvatores, WPEC, Nuclear Energy Agency, OECD 2008, Paris, France.

[6] "Assesment of the unresolved resonance treatment for cross section and covariance representation", Final report of the *NEA/WPEC-32*, NEA/NSC/WPEC/DOC(2011)430, Coordinator L. Leal, WPEC, Nuclear Energy Agency, OECD 2011, Paris, France.

[7] R. Capote, D.L. Smith, and A. Trkov, "Nuclear Data Evaluation Methodology Including Estimates of Covariances,", EPJ Web of Conferences **8**, 04001 (2010).

[8] M. Herman, R Capote, B.V. Carlson, P. Obložinský, M. Sin, A. Trkov, H. Wienke, and V. Zerkin, "EMPIRE: Nuclear Reaction Model Code System for Data Evaluation", Nucl. Data Sheets **108**, 2655–2715 (2007).

[9] D.W. Muir, "Global Assessment of Nuclear Data Requirements – the GANDR Project, An IAEA Nuclear Data Section Data Development Project ", (see *http://www-nds.iaea.org/gandr/*); D. W. Muir, A. Mengoni, and I. Kodeli, "Integration of International Standards Evaluation into a Global Data Assessment," Nucl. Data Sheets **109**, 2874–2879 (2008).

[10] R. Capote, L. Leal, Liu Ping, Liu Tingjin, P. Schillebeeckx, M. Sin, I. Sirakov, and A. Trkov, "Evaluated Nuclear Data for Nuclides within the Thorium-Uranium Fuel Cycle", Technical report *STI/PUB/1435*, ISBN 978–92–0–101010–0, International Atomic Energy Agency, Vienna, Austria (2010). (see *http://www-nds.iaea.org/publications/*).

[11] M. Chadwick, P. Obložinský, M. Herman, N. Greene, R. McKnight, D. Smith, P. Young, R. MacFarlane, G. Hale, S. Frankle, A. Kahler, T. Kawano, R. Little, D. Madland, P. Moller, R. Mosteller, P. Page, P. Talou, H. Trellue, M. White, W. Wilson, R. Arcilla, C. Dunford, S. Mughabghab, B. Pritychenko, D. Rochman, A. Sonzogni, C. Lubitz, T. Trumbull, J. Weinman, D. Brown, D. Cullen, D. Heinrichs, D. McNabb, H. Derrien, M. Dunn, N. Larson, L. Leal, A. Carlson, R. Block, J. Briggs, E. Cheng, H. Huria, M. Zerkle, K. Kozier, A. Courcelle, V. Pronyaev, and S. van der Marck, "ENDF/B-VII.0: Next generation evaluated nuclear data library for nuclear science and technology", Nucl. Data Sheets **107**, 2931–3060 (2006).

[12] R. Capote, A. Trkov, I. Kodeli, E. Soukhovitskii, L.C. Leal, M. Herman, and D.W. Muir, "Evaluation of tungsten isotopes in the fast neutron range including cross-section covariance estimation", in Proceedings of the International Conference on Nuclear Data for Science and Technology, April 22-27, 2007, Nice, France, editors O.Bersillon, F.Gunsing, E.Bauge, R.Jacqmin, and S.Leray, EDP Sciences, pp. 689–692 (2008).

[13] P. Batistoni, M. Angelone, L. Petrizzi, and M. Pillon, "Neutronics Benchmark Experiment on Tungsten", J. Nucl. Materials **329–333**, Part 1, 683–686 (2004).

[14] "ICSBEP 2006", International Handbook of Evaluated Criticality Safety Benchmark Experiments, Technical Report *NEA/NSC/DOC(95)03*, NEA Nuclear Science Committee, Nuclear Energy Agency, OECD 2006, Paris France.

[15] A. Trkov, R. Capote, I. Kodeli and L. Leal, "Evaluation of Tungsten Nuclear Reaction Data with Covariances", Nucl. Data Sheets **109**, 2905–2909 (2008) (see evaluated data files and comments at *http://www-nds.iaea.org/wolfram/*).

[16] S.F. Mughabghab, "Atlas of Neutron Resonances", Elsevier ISBN-10:0-444-52035-X, Amsterdam - Tokio (2006).

[17] H. Derrien, L.C. Leal, and N.M. Larson, "R-Matrix Analysis of $^{232}$Th Neutron Transmissions and Capture cross sections in the Energy Range Thermal to 4 keV," Nucl. Sci. & Eng. 160, 149-167 (2008).

[18] L.C. Leal, G. Arbanas, D. Wiarda and H. Derrien, "Resonance Region Covariance Analysis Method and New Covariance Data for $^{232}$Th, $^{233}$U, $^{235}$U, $^{238}$U, and $^{239}$Pu", Nucl. Data Sheets **109**, 2868-2873 (2008).

[19] C. Lampoudis, K. Guber, S. Kopecky, P. Schillebeeckx and P. Siegler, "Neutron Total and Capture Cross Section of Tungsten Isotopes ", International Conference on Nuclear Data for Science and Technology, April 26-30, 2010, Jeju Island, Korea, Journal of the Korean Physical Society, 59, 2, 1860-1863, (2011). editors O.Bersillon, F.Gunsing, E.Bauge, R.Jacqmin, and S.Leray, EDP Sciences, pp. 689–692 (2008).

[20] L. Leal *et al.*, private communication, 2010.

[21] M. Chadwick *et al.*, Nucl. Data Sheets, **112**, XXXX (2011); in this number.

[22] E.Sh. Soukhovitskii, R. Capote, J.M. Quesada and S. Chiba, "Dispersive coupled-channel analysis of nucleon scattering from $^{232}$Th up to 200 MeV", Phys. Rev. **C72**, 024604 (2005).

[23] R. Capote, M. Herman, P. Obložinský, P.G. Young, S. Goriely, T. Belgya, A.V. Ignatyuk, A.J. Koning,

S. Hilaire, V.A. Plujko, M. Avrigeanu, O. Bersillon, M.B. Chadwick, T. Fukahori, Zhigang Ge, Yinlu Han, S. Kailas, J. Kopecky, V.M. Maslov, G. Reffo, M. Sin, E.Sh. Soukhovitskii, and P. Talou, "RIPL – Reference Input Parameter Library for Calculation of Nuclear Reactions and Nuclear Data Evaluations", NUCL. DATA SHEETS **110**, 3107–3214 (2009) (see *http://www-nds.iaea.org/RIPL-3/*).

[24] T. Belgya, O. Bersillon, R. Capote, T. Fukahori, Zhigang Ge, S. Goriely, M. Herman, A.V. Ignatyuk, S. Kailas, A. Koning, V. Plujko, and P. Young, "Handbook for calculations of nuclear reaction data: Reference Input Parameter Library-2", Tech. Report *IAEA-TECDOC-1506* , International Atomic Energy Agency, Vienna, Austria (2006) (Available from *http://www-nds.iaea.org/RIPL-2/*).

[25] W. Hauser and H. Feshbach, "The Inelastic Scattering of Neutrons", PHYS. REV. **87**, 366 (1952).

[26] H. M. Hofmann, J. Richert, J. W. Tepel, and H. A. Weidenmüller, "Direct reactions and Hauser-Feshbach theory", ANN. PHYS. **90**, 403 (1975).

[27] D.L. Smith, "Covariance Matrices for Nuclear cross sections Derived from Nuclear Model Calculations", Report *ANL/NDM-159*, Argonne National Laboratory (2004).

[28] M. Herman, M.T. Pigni, P. Obložinský, S.F. Mughabghab, C.M. Mattoon, R. Capote, Young-Sik Cho, and A. Trkov, "Development of Covariance Capabilities in EMPIRE Code",NUCL. DATA SHEETS **109**, 2752–2761 (2008).

[29] T. Kawano and K. Shibata, "Covariance Evaluation System", JAERI Data/Code, Japan Atomic Energy Research Institute, Tokai, Japan, 1997.

[30] D.L. Smith, "A Unified Monte Carlo Approach to Fast Neutron Cross Section Data Evaluation", Proc. of the 8th International Topical Mtg. on Nucl. Applics. and Util. of Accelerators, Pocatello, July 29 - August 2, 2007, p.736.

[31] R. Capote and D.L. Smith, "An Investigation of the Performance of the Unified Monte Carlo Method of Neutron Cross Section Data Evaluation", NUCL. DATA SHEETS **109**, 2768–2773 (2008).

[32] R. Capote and D.L. Smith, "Unified Monte Carlo and Mixed Probability Functions", J. KOR. PHYS. SOC. 59, 1284–1287 (2011).

[33] EXchange FORmat database (EXFOR) is maintained by the Network of Nuclear Reaction Data Centers (see *http://www-nds.iaea.org/nrdc/*). Data available online (e.g. at *http://www-nds.iaea.org/exfor/*).

[34] G. Žerovnik, A. Trkov, R. Capote, D. Rochman, "Influence of resonance parameters' correlations on the resonance integral uncertainty; $^{55}$Mn case",NUCL. INST. METH. IN PHYS. RES. **A632**, 137–141 (2011).

[35] W.P. Abfalterer, F.B. Bateman, F.S. Dietrich, R.W. Finlay, R.C. Haight and G.L. Morgan, "Measurement of neutron total cross section up to 560 MeV", PHYS. REV. **C63**, 044608 (2001).

[36] F.S. Dietrich, J.D. Anderson, R.W. Bauer, S.M. Grimes, R.W. Finlay, W.P. Abfalterer, F.B. Bateman, R.C. Haight, G.L. Morgan, E. Bauge, J.P. Delaroche, and P. Romain, "Importance of isovector effects in reproducing total cross-section differences", PHYS. REV. **C67**, 044606 (2003).

[37] H. Derrien, L. C. Leal, and N. M. Larson, "New Evaluation of the $^{232}$Th Neutron Resonance Parameters in the Energy Range 0 to 4000 keV," in Proc. of PHYSOR–2006, American Nuclear Society Topical Meeting on Reactor Physics: Advances in Nuclear Analysis and Simulation, September 10–14, 2006, Vancouver, British Columbia, Canada.

[38] H. Derrien, L. C. Leal, and N. M. Larson, "R-Matrix Analysis of $^{232}$Th Neutron Transmissions and Capture Cross Sections in the Energy Range Thermal to 4 keV," NUCL. SCI. & ENG. **160**, 149–167 (2008).

[39] N. M. Larson, "Updated Users' Guide for SAMMY: Multilevel R-Matrix Fits to Neutron Data Using Bayes Equations," Tech. Report *ORNL/TM-9179/R7*, 2007.

[40] D.K. Olsen and R.W. Ingle, Measurement of neutron-transmission spectra through $^{232}$Th from 8 meV to 4 keV", Tech. Report *ORNL/TM-7661*, 1981.

[41] P. Schillebeeckx, Private Communication.

[42] F. Gunsing, Private Communication.

[43] R.E. Chrien, H.I. Liou, M.J. Kenny, and M.L. Stelts, "Neutron cross sections of $^{232}$Th", NUCL. SC. & ENG. 72, 202 (1979).

[44] W. Lundgren, "A study of the energy dependence of the $^{232}$Th capture cross section in the energy region 0.1 eV to 3.4 eV", NUKLEONIK **11**,61 (1968), EXFOR 20006.

[45] A. Trkov, Private Communication.

[46] I. Sirakov, R. Capote, F. Gunsing, P. Schillebeeckx, and A. Trkov, "An ENDF-6 compatible evaluation for neutron induced reactions of $^{232}$Th in the unresolved resonance region", ANN. NUCL. ENERGY **35**, 1223–1231 (2008).

[47] D.E. Cullen, "PREPRO 2010 - 2010 ENDF/B Pre-processing Codes", International Atomic Energy Agency, Vienna , Austria, Tech. Report *IAEA-NDS-39, Rev. 14*, October 31, 2010. (see *http://www-nds.iaea.org/ndspub/endf/prepro/*).

[48] A.Trkov and C.L. Dunford, ENDF Checking and Utility Codes. Available online at *http://www.nndc.bnl.gov/nndcscr/endf/endf-util/*.

[49] R.E. MacFarlane and A.C. Kahler, "Methods for Processing ENDF/B-VII with NJOY", NUCL. DATA SHEETS **111**, 2739–2890 (2010).

[50] V.P. Kolotov and F. De Corte, "An electronic database with compilation of $k_0$ and related data for NAA", J. RADIOAN. NUCL. CHEM. 257, 501–508 (2003). (see *http://old.iupac.org/projects/2001/2001-075-1-500.html*).

[51] D. Wiarda and M. E. Dunn, "PUFF-IV: A Code for Processing ENDF Uncertainty Data into Multigroup Covariance Matrices," Tech. Report *ORNL/TM-2006/147*, UT-Battelle, LLC, Oak Ridge National Laboratory, October 2006.

[52] H. Vonach, A. Pavlik, and B. Strohmaier, "Accurate determination of (n,2n) cross sections for haevy nuclei from neutron production spectra", NUCL. SCI. & ENG. **106**, 409–414 (1990).

[53] K.I. Zolotarev, "Evaluation of cross-section data from threshold to 40-60 MeV for specific neutron reactions important for neutron dosimetry applications", Technical report *INDC(NDS)-0546*, IAEA, Vienna, Austria (2009).

[54] J. Harvey *et al.*, "ORELA measurements", EXFOR number 13770.

[55] G. Aerts *et al.*, "GELINA measurements (unpublished)", private communication, 2006.

[56] K. Guber *et al.*, "ORELA measurements (unpublished) ", private communication, 2007.

[57] F. Widder, "Neutron capture cross-section measurements in the energy region from 0.01 to 10 electron volts",

*Eidg. Inst. Reaktorforsch. Wuerenlingen Reports* No.217, Switzerland (1975).

[58] R.E. Coté, L.M. Bollinger, and G.E. Thomas, "Neutron cross sections of Manganese", Phys. Rev. **134**, B1047–B1051 (1964).

[59] L.J. Rainwater, W.W. Havens, C.S. Wu, and J.R. Dunning, "Slow neutron velocity spectrometer studies. I. Cd, Ag, Sb, Ir, Mn", Phys. Rev. **71**, 65–79 (1947).